Effects of Sodium Ions on DNA Duplex Oligomers: Improved Predictions of Melting Temperatures

Richard Owczarzy,* Yong You, Bernardo G. Moreira, Jeffrey A. Manthey, Lingyan Huang, Mark A. Behlke, and Joseph A. Walder

Integrated DNA Technologies, 1710 Commercial Park, Coralville, Iowa 52241

Received April 18, 2003; Revised Manuscript Received January 27, 2004

ABSTRACT: Melting temperatures, T_m, were systematically studied for a set of 92 DNA duplex oligomers in a variety of sodium ion concentrations ranging from 69 mM to 1.02 M. The relationship between T_m and ln [Na^+] was nonlinear over this range of sodium ion concentrations, and the observed melting temperatures were poorly predicted by existing algorithms. A new empirical relationship was derived from UV melting data that employs a quadratic function, which better models the melting temperatures of DNA duplex oligomers as sodium ion concentration is varied. Statistical analysis shows that this improved salt correction is significantly more accurate than previously suggested algorithms and predicts salt-corrected melting temperatures with an average error of only 1.6 °C when tested against an independent validation set of T_m measurements obtained from the literature. Differential scanning calorimetry studies demonstrate that this T_m salt correction is insensitive to DNA concentration. The T_m salt correction function was found to be sequence-dependent and varied with the fraction of G·C base pairs, in agreement with previous studies of genomic and polymeric DNAs. The salt correction function is independent of oligomer length, suggesting that end-fraying and other end effects have little influence on the amount of sodium counterions released during duplex melting. The results are discussed in the context of counterion condensation theory.

Cations stabilize the duplex state of DNA.[1] The relationship between sodium ion concentration and the melting temperature (T_m) of duplex DNA has been extensively studied, and a variety of algorithms have been proposed to predict the change in T_m that occurs with changes in sodium ion concentration (*1*−*8*). To use a salt-correction algorithm, a reference melting temperature for a given sequence must either be measured or estimated by calculation using the nearest-neighbor model (*7*−*9*). Melting temperatures for short duplex DNAs are usually calculated using nearest-neighbor formulas that assume a two-state transition and typically employ 1 M monovalent cation as the reference buffer. Estimates of T_m obtained by this calculation will be most accurate when used to predict T_m in buffers that are similar to buffers originally used in the experimental systems where the nearest-neighbor thermodynamic parameters were determined. Melting temperatures are then scaled (i.e., salt-corrected) from the reference conditions to a buffer of desired composition.

Significant progress has been made in improving the nearest-neighbor and next-nearest-neighbor parameters that are used to predict T_m for DNA and RNA duplex oligomers (*7, 10*−*12*). Unfortunately, systematic studies of the salt dependence of DNA duplex thermodynamics have historically focused on long genomic DNAs (*1, 3, 5, 13*−*21, 90, 91*), repeating DNA polymers (*17, 21, 22*), plasmids, and long restriction enzyme fragments (*4, 14, 20*). Long DNAs are unlikely to melt in a two-state fashion, so interpreting thermodynamic studies on these molecules can obscure some trends that might otherwise be apparent using shorter sequences. Several investigators have reported the salt effects on T_m's for short synthetic DNA hairpins (*23, 24*), dumbbells (*12, 25*−*27*), and 6−30 base pair long oligomers (*8, 24, 26, 28*−*42, 66*). Even if taken together, these prior works do not constitute a sufficiently large data set to model the salt dependence of T_m for short (6−50 base pairs) DNA duplex oligomers. A need for more extensive experimental thermodynamic data for DNA oligomers was pointed out in a recent review (*43*).

Modern experimental molecular biology relies upon the enormous selectivity that can be achieved in DNA hybridization events. Accurate and specific hybridization of synthetic oligonucleotides in the range from 10 to 50 base pairs is required to perform a wide variety of techniques, such as DNA sequencing or PCR amplification (*2, 44*). The successful implementation of these techniques is dependent upon the use of nucleic acid probes and primers that specifically hybridize with complementary nucleic acids of interest while, at the same time, avoid nonspecific hybridization with other nucleic acid molecules that may be present. Widespread use of these techniques is further dependent upon the availability of good predictive algorithms that allow design of oligonucleotide sequences and reaction conditions that work well without the need to empirically test each DNA sequence used as a primer. Current design algorithms typically estimate primer T_m using the nearest-neighbor model (*7, 8*) for conditions of 1 M NaCl and then scale this estimate to the

* To whom correspondence should be addressed. Phone: (319) 626-8459. E-mail: science@owczarzy.net. Internet: http://www.owczarzy.net

[1] Abbreviations: DNA, deoxyribonucleic acid; DSC, differential scanning calorimetry; CE, capillary electrophoresis; PCR, polymerase chain reaction; UV, ultraviolet.

10.1021/bi034621r CCC: $27.50
Published on Web 03/05/2004

buffer conditions employed in the actual biochemical reaction, where the monovalent cation concentration is often around 50 mM. If present, divalent cations will also affect T_m and will need to be taken into consideration. Any errors in the salt correction calculation can result in failed reactions or in reactions that have poor specificity. Further, these errors become additive in applications that require many oligonucleotides reacting together, such as multiplex PCR or microarrays. Therefore, while acceptable results may be obtained using predictive programs for singlet reactions, most multiplex reactions still require empiric optimization. To improve predictions of melting temperatures for short DNA duplex oligomers, we investigated the dependence of DNA thermal stability on monovalent cation concentration for a large set of sequences in a variety of sodium ion concentrations.

We conducted melting experiments for a set of 92 DNA duplex oligomers that ranged in length from 10 to 30 base pairs and varied in G·C base pair content from 20% to 80%. Molecules were designed to systematically evaluate the effects of both oligomer sequence and length. A total of over 2700 melting profiles were collected in buffers of sodium ion concentrations ranging from 69 mM to 1 M. We found that the observed melting temperatures were not well predicted by preexisting algorithms (*1*−*7*). New algorithms were obtained that better fit the experimental data. We propose a new general empirical equation (eq 22), which can be used to more accurately scale melting temperatures of DNA duplex oligomers between environments of various sodium ion concentrations. We statistically analyze and compare accuracy of our empirical equation with accuracy of other published T_m salt corrections. We also consider possible explanations for the experimental observations in terms of potential molecular events that are consistent with our thermodynamic data in the context of counterion condensation theory.

MATERIALS AND METHODS

DNA Synthesis and Purification. DNA single-strand oligomers were synthesized using solid-phase phosphoramidite chemistry, and each had an OH group on the 5′-end, as well as on the 3′-end. Oligomers were purified by 20% polyacrylamide−7 M urea denaturing gel electrophoresis. Technical details of purification procedures and tests of oligomer quality have been published elsewhere (*45*). The purity of each oligomer was assessed by capillary electrophoresis (CE) on a Beckman PACE 5000 (Beckman Coulter, Fullerton, CA). All oligomers used were at least 92% pure by CE. Oligomer identity was verified by mass spectrometry using a delayed extraction matrix-assisted laser desorption ionization time-of-flight mass spectrometer (DE-MALDI TOF) on a Voyager DEJ Biospectrometry workstation (Applied Biosystems Inc, Foster City, CA). Relative molecular masses of all oligomers were within 0.4% of expected molecular mass.

Optical Melting Studies. Inorganic reagents were at least 99.5% pure and were purchased from Sigma-Aldrich or Amresco. Melting experiments were carried out in buffers containing 3.87 mM NaH_2PO_4, 6.13 mM Na_2HPO_4, 1 mM Na_2EDTA, and 50, 100, 200, 600, or 1000 mM NaCl, adjusted to pH 7.0 ± 0.03 with 1 M NaOH. Total final Na^+ concentrations were 68.9, 119, 220, and 621 mM and 1.02 M, respectively. DNA samples were dialyzed against melting buffers in either Quix Sep microdialyzers (Membrane Filtration Products, Seguin, TX) or a 28-Well Microdialysis System (Invitrogen, Carlsbad, CA) and filtered through a 0.45 μm nylon filter. Concentrations of single-strand oligomers were determined from absorbance at 260 nm and estimated extinction coefficients that were calculated using the nearest-neighbor model (*46*, *47*). Oligomer concentrations were estimated at least twice for each sample using different dilutions. If these concentrations for any sample differed by more than 4%, the results were discarded and measurements were repeated. To prepare DNA duplexes, complementary oligomers were mixed in 1:1 molar ratios, heated to 94 °C, and slowly cooled to ambient temperature.

Melting experiments were conducted on a single beam Beckman DU 650 spectrophotometer with a Micro Tm Analysis accessory, a Beckman High Performance Peltier controller, and either 1 cm or 1 mm path-length cuvettes (Beckman Coulter, Fullerton, CA). Beckman software was reprogrammed so that absorbance values at 268 nm were monitored every 0.1 °C in the temperature range of 10−95 °C. Both heating (denaturation) and cooling (renaturation) transition curves were recorded at a controlled rate of temperature change of 24.9 ± 0.3 °C/h. Temperatures, which were previously shown (*45*) to be identical to temperatures of the DNA solutions within the experimental error of melting temperatures ($\sigma_{T_m} = 0.3$ °C), were measured by an internal probe located inside the Peltier holder.

Melting experiments were analyzed as described earlier (*8*, *25*). The absorbance data were not corrected for volume expansion of solutions with increasing temperatures. Melting profiles of buffers alone were subtracted from the raw absorbance versus temperature curves of DNA samples. The regions of linear increase of absorbance before and after the melting transition were least-squares fit to lower and upper baselines (see Figure 2 in ref 48). The fraction of broken base pairs was calculated from the standard formula, $\theta = (A - A_L)/(A_U - A_L)$, where A, A_L, and A_U are sample absorbance, absorbance of the lower baseline, and absorbance of the upper baseline, respectively (*48*). Melting curves were smoothed by a digital filter (*49*). Reported transition (melting) temperatures are temperatures at the midpoint of the transitions where $\theta = 0.5$, where half of the base pairs are broken (melted). Three to eight melting curves were collected for each DNA duplex oligomer in different cuvettes and different positions inside of the Peltier holder to minimize systematic errors.

Differential Scanning Calorimetry (DSC) Studies. Measurements were performed using a Nano II differential scanning calorimeter (Calorimetry Sciences Corporation, American Fork, UT). Dialyzed concentrated DNA stock samples in 69 mM Na^+ buffer were diluted to the same DNA duplex concentrations ($C_t = 180$ μM) and degassed for 17 min at 25 mmHg using the vacuum system supplied with the calorimeter. Weight measurements indicated that less than 1.3% of the buffer evaporated during degassing. Typically, the buffer vs buffer scan was collected twice, and the sample cell was then emptied and loaded with the DNA duplex sample. Each DNA oligomer was scanned up and down twice at a heating rate of 1 °C/min to verify reproducibility of the melting curves. Samples were recovered from calorimetric

cells, lyophilized in a Speed-Vac concentrator, dialyzed against 1 M Na^+ melting buffer and run again. For each DSC experiment, DNA concentrations were determined from absorbance of 100× diluted calorimetric samples at 260 nm and 85 °C before and after the calorimetric run. Melting data were analyzed using the CpCalc, v2.1, package supplied by the manufacturer and the standard published procedure (*50*). The excess heat capacity curve, ΔC_p^{exc}, versus temperature, was obtained by subtraction of the buffer versus buffer scan from the sample versus buffer scan. Differences between pretransition and posttransition baselines on the graph of excess heat capacity were negligible. Reported DSC melting temperatures are temperatures at peak height maxima on excess heat capacity vs temperature curves. Integrated areas under these curves provided calorimetric transition enthalpies,

$$\Delta H_{DSC} = \int \Delta C_p^{exc}\, dT \quad (1)$$

We wanted to obtain a set of DSC melting temperatures at the same DNA concentration in buffers of two different Na^+ concentrations. In 69 mM Na^+ buffer, DSC experiments were conducted at $C_t = 180\ \mu M$. As described above, DSC experiments in 1 M Na^+ melting buffer were conducted at slightly lower DNA concentrations ($C_t = 148\ \mu M$ on average). To determine DSC melting temperatures, T_m^0, at our standard $C_t = 180\ \mu M$ and in 1 M Na^+ buffer from experimental melting temperatures, T_m^1, measured at slightly lower concentrations, C_t^1, the following relationship derived from the van't Hoff equation was employed (*51*):

$$\frac{1}{T_m^0} = \frac{1}{T_m^1} + \frac{R}{\Delta H_{DSC}} \ln\left[\frac{180 \times 10^{-6}}{C_t^1}\right] \quad (2)$$

where ΔH_{DSC} is the experimentally measured calorimetric enthalpy in 1 M Na^+ buffer and R is the ideal gas constant. We assume in these calculations that ΔH_{DSC} does not change between T_m^0 and T_m^1. Since the average difference between T_m^0 and T_m^1 is only 0.3 °C for our calorimetric data set, any error introduced by this assumption is negligible and will not significantly influence the outcome of calculations.

Statistical Analysis of T_m Predictions. Quality and goodness-of-fit of various T_m salt corrections were assessed from average errors of T_m predictions, $|\langle T_m \rangle|_{AVE}$, and reduced χ_r^2. For a set of M experimentally measured melting temperatures, T_m(experiment,i), melting temperatures were predicted, T_m(prediction,i), and the following formulas were employed:

$$|\langle T_m \rangle|_{AVE} = \frac{\sum_{i=1}^{i=M} |T_m(\text{prediction},i) - T_m(\text{experiment},i)|}{M} \quad (3)$$

$$\chi_r^2 = \frac{1}{\nu} \frac{\sum_{i=1}^{i=M} [T_m(\text{prediction},i) - T_m(\text{experiment},i)]^2}{\sigma_{T_m}^2} \quad (4)$$

where $|T_m(\text{prediction},i) - T_m(\text{experiment},i)|$ is the absolute value of the difference between predicted and measured melting temperatures, ν is the number of degrees of freedom, and σ_{T_m} is the experimental standard deviation of melting temperatures. Reduced χ_r^2 for various T_m salt corrections were compared to evaluate whether the corrections are significantly different in their errors of T_m predictions. *F*-test ratios between each salt correction j and salt correction k were calculated,

$$F = \frac{\chi_r^2(j)}{\chi_r^2(k)} \quad (5)$$

Probabilities, $P(j,k)$, of null hypothesis that observed differences in $\chi_r^2(j)$ and $\chi_r^2(k)$ were insignificant and could happen by random chance alone were evaluated from these ratios by the incomplete beta function, I, (*52*, *53*)

$$P(j,k) = I_{\nu_k/(\nu_k+\nu_j F)}\left(\frac{\nu_k}{2}, \frac{\nu_j}{2}\right) \quad (6)$$

where ν_j and ν_k were the number of degrees of freedom for the salt corrections j and k, respectively. The smaller the $P(j,k)$ probability is, the more significant the difference between two salt corrections is. If such probabilities were less than 5%, the null hypothesis was rejected, and the salt corrections were deemed to exhibit significantly different goodness-of-fit and accuracies of T_m predictions. The probabilities were calculated by function @BETAI in Corel Quattro Pro. This analysis assumes that errors of melting data were normally distributed.

RESULTS AND DISCUSSION

Survey of Published T_m Salt Corrections. Since the first pioneering experiments done over 40 years ago (*15*, *54*, *55*), numerous nucleic acid helix−coil melting transitions have been reported. Several different equations have been offered to model the effects that monovalent cations have on melting temperatures and stability of duplex DNAs. To our knowledge, Table 1 lists all previously published T_m salt corrections for duplex DNAs. Many of these corrections were derived from melting experiments using genomic and polymeric DNAs. In 1965, Schildkraut and Lifson (*1*) observed that the T_m of sheared *Escherichia coli* DNA in a buffered solution is proportional to the logarithm of sodium ion concentrations in the range of 0.01−0.20 M Na^+ and reported that eq 7, shown in the first row of Table 1, accurately modeled this relationship. Almost 40 years later, this equation remains the most frequently used T_m salt correction in molecular biology primer-design and DNA-hybridization modeling software (*56*−*62*). Unfortunately, a broad misunderstanding of the limitations for eq 7 persists; an equation that was developed to model the melting behavior of a specific bacterial genomic DNA sequence within a narrow range of sodium ion concentrations is still being routinely applied to model the behavior of short DNA oligomers of any base composition in a wider range of ionic environments with no evidence to support that such generalizations are valid. Wetmur later modified eq 7 and suggested an improved salt correction (eq 8) that better models T_m in environments of high sodium ion concentrations (*2*). Again, little experimental evidence has been published that shows whether this new relationship improves the T_m salt correction for short DNA oligomers used in molecular biology applications.

Table 1: The Previously Published Salt Corrections for Melting Temperatures of DNA Duplex Oligomers and Polymers

number	name	ref	equation
7	Schildkraut−Lifson equation	*1*	$T_m(2) = T_m(1) + 16.6 \log \frac{[Na^+]_2}{[Na^+]_1}$
8	Wetmur salt correction	*2*	$T_m(2) = T_m(1) + 16.6 \log \frac{[Na^+]_2(1 + 0.7[Na^+]_1)}{(1 + 0.7[Na^+]_2)[Na^+]_1}$
9	Frank-Kamenetskii equation	*3*	$T_m(2) = T_m(1) + (7.95 - 3.06f(G{\cdot}C)) \ln \frac{[Na^+]_2}{[Na^+]_1}$
10	Marmur−Schildkraut−Doty equation	*4, 5*	$T_m(2) = T_m(1) + (8.75 - 2.83f(G{\cdot}C)) \ln \frac{[Na^+]_2}{[Na^+]_1}$
11	Blake−Delcourt nearest-neighbor salt correction	*4*	$T_m(2) = T_m(1) + \sum_{ij}\left(\left(\frac{dT_m}{d \log [Na^+]}\right)_{ij}\frac{N_{ij}}{\sum_{ij}N_{ij}}\right) \log \frac{[Na^+]_2}{[Na^+]_1}$
12	$T_m - 12.5 \log [Na^+]$ salt correction	*6*	$T_m(2) = T_m(1) + 12.5 \log \frac{[Na^+]_2}{[Na^+]_1}$
13	SantaLucia unified parameters[a]	*7*	$\frac{1}{T_m(2)} = \frac{1}{T_m(1)} + \frac{0.368N}{\Delta H^\circ} \ln \frac{[Na^+]_2}{[Na^+]_1}$
14	Owczarzy−Vallone−Gallo−Paner−Lane−Benight salt correction[b]	*8*	$T_m(115\ mM\ Na^+) = T_m(1\ M\ Na^+) + (8.91f(G{\cdot}C) - 11.34)$

[a] DNA oligomers in our work do not have any terminal phosphates; therefore, $N = N_{bp} - 1$. [b] Salt correction only between two specific buffers containing 1 M and 115 mM Na^+ was reported.

Melting experiments done on a larger set of genomic bacterial DNAs suggested that the T_m salt correction function may be sequence-dependent. Frank-Kamenetskii (*3*) has reanalyzed the melting data from Owen et al. (*13*) and proposed a T_m salt correction (eq 9) where the effects of salts on DNA melting temperatures depend on the fraction of G·C base pairs, f(G·C). A similar relationship was proposed by Marmur, Doty, and Schildkraut (*4, 5*) in a revised T_m salt correction (eq 10). Blake and Delcourt (*4*) measured melting transitions of synthetic tandem-repeat DNAs inserted in recombinant pN/MCS plasmids over the range 0.034−0.114 M Na^+. They observed that the change of T_m as a function of log [Na^+] varies with sequence and reported 10 nearest-neighbor dT_m/dlog [Na^+] parameters that could be used to calculate the salt-corrected T_m's of duplex DNAs from eq 11. The nearest-neighbor parameters, $(dT_m/d \log [Na^+])_{ij}$, are multiplied by fractions of each nearest-neighbor ij, $N_{ij}/(\sum N_{ij})$, where N_{ij} is the number of times the particular ij doublet (for example, 5′-AC-3′/5′-GT-3′) is present in a oligomer sequence. The sums in eq 11 are calculated over all 10 nearest-neighbor parameters.

Recently, three new T_m salt corrections have been proposed that were derived from melting experiments using DNA oligomers. In 1996, SantaLucia et al. published a new set of nearest-neighbor DNA parameters (*6*) and proposed relationship 12 for use as a salt correction for DNA oligomers with the limitation that this equation may not apply in ionic environments below 0.1 M Na^+. This correction additionally assumed that trends in nearest-neighbor stability are independent of salt concentrations. More recently, SantaLucia reported a "unified nearest-neighbor parameter set" (*7, 63*) with an improved T_m salt correction formula (eq 13). Here, salt dependence was presumed to be entirely entropic, that is, transition enthalpies, ΔH°, were assumed to be salt-concentration-independent. Equation 13 was derived from the literature data for 26 oligonucleotide duplexes in 0.01−0.3 M NaCl buffers. Finally, Owczarzy et al. (*8*) investigated melting behavior of 16 DNA oligomers with varying G·C content in two sodium ion concentrations, 1 M and 115 mM. Expression 14 was derived for T_m corrections between those two ionic environments. This T_m salt correction was found to be dependent on the fraction of G·C base pairs. Unfortunately, the relatively small data set employed did not permit this T_m salt correction to be generalized for use with buffers of a wider variety of ionic concentrations. In summary, eight different equations have been proposed to model the relationship between T_m and monovalent salt concentration. No clear consensus exists as to the limitations and accuracy of the various T_m salt corrections or their utility in predicting T_m outside the range of sodium ion concentrations studied. Furthermore, it is not clear whether T_m salt corrections derived using genomic and long polymeric DNAs can be directly applied to short DNA duplex oligomers.

Dependence of DNA Duplex Thermal Stability on Sodium Ion Concentrations. DNA sequences and their experimental melting temperatures in five different ionic environments (69, 119, 220 and 621 mM and 1.02 M Na^+) are reported in Table 2. All DNA molecules were annealed to form non-self-complementary duplexes and range in numbers of base pairs, N_{bp}, from 10 to 30. Their mole fractions of G·C base pairs, f(G·C), varied from 0.2 to 0.8. The sequences were designed to anneal into intact blunt-end duplexes and avoid self-dimer, hairpin, or other competing structures. Sequences with long regions of only G·C or A·T base pairs were excluded from the set to reduce non-two-state melting behavior. As a control for the accuracy and comparability of our measurements, two sequences that were previously studied by others and reported in the literature were also studied here (*6, 42*). Melting temperatures and calorimetric transition enthalpies for those two oligomers showed excellent reproducibility and no significant systematic errors in temperature calibrations of our equipment (data not shown). Figure 1 shows representa-

Table 2: Experimentally Measured UV Melting Temperatures of DNA Duplex Oligomers in Buffers of Various Na^+ Concentrations

DNA sequence (5′ to 3′)	*f*(G•C)	T_m (°C) at total [Na^+] indicated[a]				
		69 mM	119 mM	220 mM	621 mM	1.02 M
		10,11-mers				
ATCAATCATA	0.20	21.3	24.5	27.9	32.4	33.6
TTGTAGTCAT	0.30	24.7	28.2	31.2	34.8	36.0
GAAATGAAAG	0.30	22.1	25.3	29.1	33.1	34.4
CCAACTTCTT	0.40	29.0	32.1	35.9	39.6	40.6
ATCGTCTGGA	0.50	33.8	37.4	40.5	44.5	44.9
AGCGTAAGTC	0.50	27.4	31.2	34.6	39.5	40.3
CGATCTGCGA	0.60	39.2	42.3	45.6	48.4	49.1
TGGCGAGCAC	0.70	44.4	47.8	51.3	55.0	55.3
GATGCGCTCG	0.70	44.2	47.0	50.1	53.6	53.5
GGGACCGCCT	0.80	46.7	50.3	53.1	56.5	57.0
CGTACACATGC[b]	0.55	40.4	43.5	46.1	49.6	49.9
CCATTGCTACC[b]	0.55	38.0	41.7	44.5	47.9	48.9
		15-mers				
TACTAACATTAACTA	0.20	35.3	40.4	44.1	49.3	51.1
ATACTTACTGATTAG	0.27	38.1	41.4	45.0	49.9	51.5
GTACACTGTCTTATA	0.33	41.0	44.8	48.3	52.9	54.8
GTATGAGAGACTTTA	0.33	39.9	44.2	47.9	53.3	55.4
TTCTACCTATGTGAT	0.33	40.6	44.6	48.1	52.3	53.7
AGTAGTAATCACACC	0.40	44.3	47.8	51.6	56.2	57.1
ATCGTCTCGGTATAA	0.40	45.5	49.4	52.9	57.4	58.6
ACGACAGGTTTACCA	0.47	47.8	51.2	55.5	59.8	61.3
CTTTCATGTCCGCAT	0.47	49.9	53.9	57.1	61.4	62.8
TGGATGTGTGAACAC	0.47	46.5	51.6	54.6	59.1	60.4
ACCCCGCAATACATG	0.53	51.3	55.2	58.5	62.4	62.9
GCAGTGGATGTGAGA	0.53	51.2	54.8	58.0	61.7	63.3
GGTCCTTACTTGGTG	0.53	47.8	51.6	55.1	59.1	60.3
CGCCTCATGCTCATC	0.60	52.8	56.7	60.1	63.6	65.8
AAATAGCCGGGCCGC	0.67	59.0	62.2	65.3	69.0	70.4
CCAGCCAGTCTCTCC	0.67	54.1	58.0	61.5	65.1	66.7
GACGACAAGACCGCG	0.67	57.9	61.5	64.4	67.6	68.6
CAGCCTCGTCGCAGC	0.73	60.8	64.1	67.4	70.1	72.0
CTCGCGGTCGAAGCG	0.73	61.5	64.6	67.1	70.0	70.7
GCGTCGGTCCGGGCT	0.80	64.9	67.7	70.5	73.9	74.1
		20-mers				
TATGTATATTTTGTAATCAG	0.20	44.4	47.7	52.6	57.6	61.2
TTCAAGTTAAACATTCTATC	0.25	45.7	49.5	53.9	59.4	61.5
TGATTCTACCTATGTGATTT	0.30	49.1	53.5	57.4	62.3	64.4
GAGATTGTTTCCCTTTCAAA	0.35	49.3	52.8	57.6	62.6	65.3
ATGCAATGCTACATATTCGC	0.40	55.2	59.5	62.9	67.0	68.9
CCACTATACCATCTATGTAC	0.40	51.1	54.6	58.4	62.2	64.4
CCATCATTGTGTCTACCTCA	0.45	55.6	59.5	63.1	67.3	68.5
CGGGACCAACTAAAGGAAAT	0.45	53.7	57.7	61.7	66.7	68.5
TAGTGGCGATTAGATTCTGC	0.45	57.0	60.6	64.8	69.1	71.2
AGCTGCAGTGGATGTGAGAA	0.50	59.7	63.5	67.6	71.3	73.1
TACTTCCAGTGCTCAGCGTA	0.50	60.3	64.4	67.7	71.6	73.6
CAGTGAGACAGCAATGGTCG	0.55	59.8	63.5	67.0	71.1	72.5
CGAGCTTATCCCTATCCCTC	0.55	56.0	60.2	64.1	68.5	70.3
CGTACTAGCGTTGGTCATGG	0.55	59.6	63.1	66.6	70.5	71.1
AAGGCGAGTCAGGCTCAGTG	0.60	64.5	67.7	71.4	75.1	76.3
ACCGACGACGCTGATCCGAT	0.60	66.0	69.1	72.6	76.8	77.3
AGCAGTCCGCCACACCCTGA	0.65	66.5	69.9	74.0	76.9	78.5
CAGCCTCGTTCGCACAGCCC	0.70	67.2	70.7	74.0	77.7	78.1
GTGGTGGGCCGTGCGCTCTG	0.75	69.2	72.7	76.2	79.6	81.0
GTCCACGCCCGGTGCGACGG	0.80	70.9	73.9	77.3	79.8	81.1
		25-mers				
GATATAGCAAAATTCTAAGTTAATA	0.20	49.1	53.5	57.7	63.3	66.1
ATAACTTTACGTGTGTGACCTATTA	0.32	56.6	60.7	64.7	69.6	71.8
GTTCTATACTCTTGAAGTTGATTAC	0.32	52.7	56.1	60.6	66.1	67.7
CCCTGCACTTTAACTGAATTGTTTA	0.36	57.4	61.4	65.6	70.1	72.5
TAACCATACTGAATACCTTTTGACG	0.36	56.5	60.2	64.3	68.9	71.3
TCCACACGGTAGTAAAATTAGGCTT	0.40	59.3	63.1	67.3	71.8	73.8
TTCCAAAAGGAGTTATGAGTTGCGA	0.40	59.1	63.0	67.2	71.6	73.8
AATATCTCTCATGCGCCAAGCTACA	0.44	62.1	65.7	70.3	75.1	76.5
TAGTATATCGCAGCATCATACAGGC	0.44	61.2	64.7	69.1	72.8	75.0
TGGATTCTACTCAACCTTAGTCTGG	0.44	59.0	63.1	67.1	71.3	73.6
CGGAATCCATGTTACTTCGGCTATC	0.48	60.9	64.7	68.7	73.3	74.8
CTGGTCTGGATCTGAGAACTTCAGG	0.52	62.1	65.8	69.6	74.2	75.6
ACAGCGAATGGACCTACGTGGCCTT	0.56	68.1	72.1	76.0	79.4	81.0
AGCAAGTCGAGCAGGGCCTACGTTT	0.56	68.3	72.6	76.3	80.0	81.5

Table 2: (Continued)

DNA sequence (5′ to 3′)	*f*(G·C)	T_m (°C) at total [Na^+] indicated[a]				
		69 mM	119 mM	220 mM	621 mM	1.02 M
25-mers (Continued)						
GCGAGCGACAGGTTACTTGGCTGAT	0.56	67.0	70.8	74.7	78.6	80.1
AAAGGTGTCGCGGAGAGTCGTGCTG	0.60	69.6	73.6	77.4	81.2	82.4
ATGGGTGGGAGCCTCGGTAGCAGCC	0.68	70.7	74.5	78.2	81.6	83.4
CAGTGGGCTCCTGGGCGTGCTGGTC	0.72	72.0	75.6	79.2	82.6	83.4
GCCAACTCCGTCGCCGTTCGTGCGC	0.72	73.5	76.5	80.6	83.2	84.6
ACGGGTCCCCGCACCGCACCGCCAG	0.80	76.8	79.9	84.0	87.1	88.3
30-mers						
TTATGTATTAAGTTATATAGTAGTAGTAGT	0.20	50.7	55.0	59.3	65.1	66.6
ATTGATATCCTTTTCTATTCATCTTTCATT	0.23	53.5	58.3	62.3	68.6	70.4
AAAGTACATCAACATAGAGAATTGCATTTC	0.30	58.3	61.9	66.1	71.3	73.2
CTTAAGATATGAGAACTTCAACTAATGTGT	0.30	56.8	61.3	64.9	70.5	71.8
CTCAACTTGCGGTAAATAAATCGCTTAATC	0.37	60.9	64.8	68.7	74.4	75.5
TATTGAGAACAAGTGTCCGATTAGCAGAAA	0.37	61.3	65.4	69.6	74.8	76.4
GTCATACGACTGAGTGCAACATTGTTCAAA	0.40	62.7	66.8	70.8	75.9	76.9
AACCTGCAACATGGAGTTTTTGTCTCATGC	0.43	64.5	68.3	72.5	77.7	78.7
CCGTGCGGTGTGTACGTTTTATTCATCATA	0.43	63.9	68.3	71.8	76.5	77.6
GTTCACGTCCGAAAGCTCGAAAAAGGATAC	0.47	64.3	68.2	72.1	77.1	78.7
AGTCTGGTCTGGATCTGAGAACTTCAGGCT	0.50	66.3	70.4	74.5	78.8	80.6
TCGGAGAAATCACTGAGCTGCCTGAGAAGA	0.50	66.3	70.4	74.1	79.0	80.9
CTTCAACGGATCAGGTAGGACTGTGGTGGG	0.57	67.6	71.7	74.7	78.8	80.1
ACGCCCACAGGATTAGGCTGGCCCACATTG	0.60	71.3	74.7	78.5	82.7	84.0
GTTATTCCGCAGTCCGATGGCAGCAGGCTC	0.60	70.6	74.9	78.1	82.4	84.1
TCAGTAGGCGTGACGCAGAGCTGGCGATGG	0.63	72.2	75.7	79.3	83.3	84.6
CGCGCCACGTGTGATCTACAGCCGTTCGGC	0.67	72.7	76.3	79.5	83.4	84.5
GACCTGACGTGGACCGCTCCTGGGCGTGGT	0.70	74.4	78.4	81.5	85.2	86.4
GCCCCTCCACTGGCCGACGGCAGCAGGCTC	0.77	76.3	79.8	83.6	87.1	87.7
CGCCGCTGCCGACTGGAGGAGCGCGGGACG	0.80	77.8	81.6	84.6	87.7	88.6

[a] All UV experiments were conducted at the same total single-strand concentrations, $C_t = (2 \pm 0.2)\ \mu M$. [b] These duplexes were also melted in other laboratories (*6, 42*).

tive melting curves of duplex DNAs for oligomers of various length. All studied duplexes displayed sharp, sigmoidal, apparently two-state transitions, although the transitions became slightly less symmetrical with increasing N_{bp}. Some melting profiles of oligomers longer than 20 base pairs had a small pretransition shoulder, which we attribute to minor deviation from the two-state model. All such deviations were small and should not significantly affect the T_m analysis. As expected, the width of melting transitions decreased with increasing N_{bp}, and in all cases, the T_m was easily identified. Within experimental error, denaturation and renaturation transition curves for all 92 DNA duplex oligomers overlapped. This observation indicates that equilibrium conditions were present throughout melting transitions (*45*). Experimental T_m's were reproducible within 0.3 °C, even between repeated melting experiments of a particular DNA sequence over a period of two years and when different synthesis lots of oligomers were compared.

Melting temperatures and their reciprocal values were plotted against the logarithm of sodium ion concentration for all 92 duplexes. Figure 2 shows representative examples of such graphs for oligomers of different lengths and G·C base pair content. The plots exhibit nonlinear dependence throughout the range of sodium ion concentrations studied. Plot curvature is greater for oligomers with high *f*(G·C). These results are consistent with a previous study (*40*), which examined solvent effects on T_m of a $(dG{\cdot}dC)_3$ duplex, where a significant increase in T_m was observed up to 0.2 M Na^+ with essentially constant T_m in buffers from 0.2 to 1.0 M Na^+. This curvature may not be apparent for plots made from a more limited data set; similar graphs have previously been fit to a linear function, and any trends toward curvature were attributed to experimental error. The possibility that T_m or $1/T_m$ may not be linearly dependent on ln [Na^+] was also suggested by Bond et al. (*93*). Careful inspections of the plots for the entire set of 92 duplex DNAs reveal that all duplexes exhibit a similar trend and curvature reproducibly occurs in the same direction. Thus, linear fits of these plots appear not to be adequate within the experimental errors of T_m.

We fitted melting temperatures using both linear and quadratic functions in a fashion similar to Bond et al. (eqs 8a−8d) (*93*). We report statistical tests to examine the goodness-of-fit for both functions. Specifically, melting temperatures as a function of sodium ion concentrations for each oligomer g from Table 2 were fit to each of the following general equations:

$$T_m = A_1(g) + B_1(g) \ln [Na^+] \quad (15)$$

$$\frac{1}{T_m} = A_2(g) + B_2(g) \ln [Na^+] \quad (16)$$

$$T_m = A_3(g) + B_3(g) \ln [Na^+] + C_3(g) \ln^2 [Na^+] \quad (17)$$

$$\frac{1}{T_m} = A_4(g) + B_4(g) \ln [Na^+] + C_4(g) \ln^2 [Na^+] \quad (18)$$

Melting temperatures were weighted equally in our regression calculations. In other words, experimentally measured uncertainties of each melting temperature were not used, because the uncertainty reflects the reproducibility but not the accuracy of the particular T_m. Figure 3 shows coefficients $B_3(g)$ and $C_3(g)$ and Figure 4 shows coefficients $B_4(g)$ and

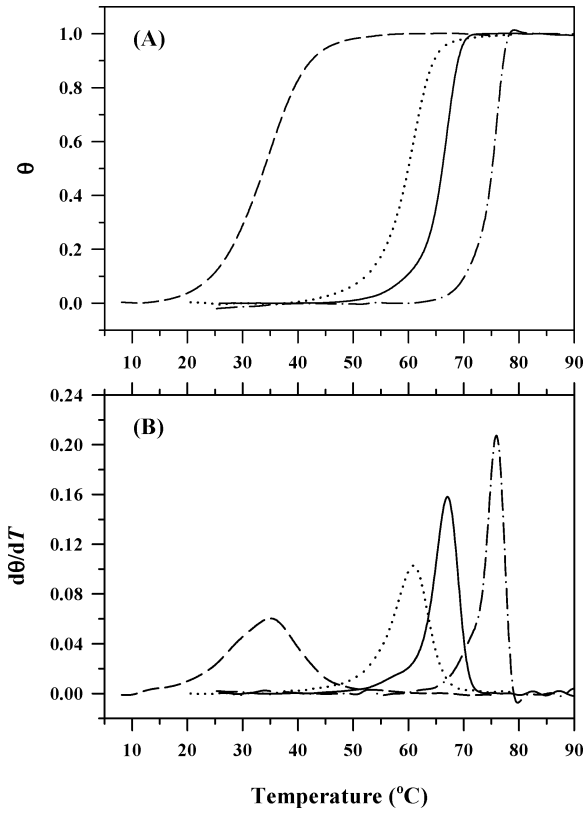

FIGURE 1: UV melting profiles (A) and derivative melting profiles (B) with respect to temperature of selected DNA duplex oligomers (f(G·C) ≈ 0.5) in 69 mM Na^+ buffer. Oligomer length is increasing from left to right: 10-mer, ATCGTCTGGA (− − −); 20-mer, TACTTCCAGTGCTCAGCGTA (···); 30-mer, TCGGAGAAATCACTGAGCTGCCTGAGAAGA (—); 60-mer, CGGAGAGGGACAGCTAGTGCCCCTGTGGGGAGTCGCTTATACAAAGCGGAGTGCAATTTT (− · −).

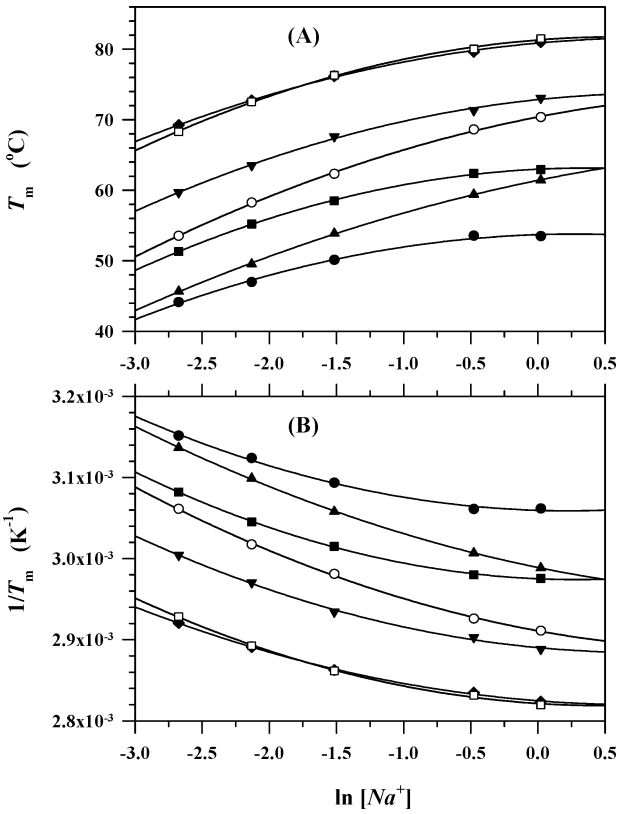

FIGURE 2: Melting temperatures (A) and reciprocal melting temperatures (B) plotted vs ln [Na^+] for representative DNA duplex oligomers of different lengths and G·C base pair contents: (●) 10-mer, 70% GC, 5′-GATGCGCTCG-3′; (■) 15-mer, 53% GC, 5′-ACCCCGCAATACATG-3′; (▲) 20-mer, 25% GC, 5′-TTCAAGTTAAACATTCTATC-3′; (▼) 20-mer, 50% GC, 5′-AGCTGCAGTGGATGTGAGAA-3′; (◆) 20-mer, 75% GC, 5′-GTGGTGGGCCGTGCGCTCTG-3′; (□) 25-mer, 56% GC, 5′-AGCAAGTCGAGCAGGGCCTACGTTT-3′; (○) 30-mer, 23% GC, 5′-ATTGATATCCTTTTCTATTCATCTTTCATT-3′. Graphs for all oligomers in our data set exhibit curvature in the same direction. However, the extent of the curvature is sequence-dependent.

$C_4(g)$ obtained from fits using eqs 17 and 18, respectively, for our set of 92 DNA duplexes. Similar plots were generated for eqs 15 and 16 in which there is only a linear term in ln [Na^+] (plots not shown). Standard deviations for the coefficients in each equation 15−18, $A_i(g)$, $B_i(g)$, $C_i(g)$, and $i = 1$, 2, 3, and 4, were evaluated by error propagation (*52*).

We found that the coefficients $B_i(g)$ for all four equations were independent of oligomer length and that the values of $C_i(g)$ were independent of both oligomer length and base composition for eqs 17 and 18 (see Figures 3 and 4). Thus, the T_m salt corrections are insensitive to the number of base pairs. This trend can be seen in Figures 3c and 4c, where slopes are plotted as a function of f(G·C). To more clearly demonstrate this relationship, d(1/T_m)/d log [Na^+] was plotted as a function of N_{bp} for six sets of DNA duplex oligomers of different G·C content (Figure 5). Within the size range studied, 10−30 base pairs, d(1/T_m)/d log [Na^+] is independent of oligomer length for duplexes of similar value of f(G·C).

The coefficients $B_i(g)$ are sequence-dependent and, to a first approximation, are proportional to the fractions of G·C base pairs (see Figures 3 and 4). Therefore the coefficients $B_i(g)$ were least-squared fit in terms of fractions of G·C and A·T base pairs to linear functions $B_i(g) = r_i f$(A·T) + $s_i f$(G·C), where r_i and s_i are two evaluated parameters for each of the eqs 15−18 (i varies from 1 to 4) and f(A·T) = 1 − f(G·C). The coefficients $B_i(g)$ were weighted equally in this fitting analysis. The parameter r_i is the coefficient B_i for duplexes containing only A·T base pairs. The parameter s_i is the coefficient B_i for duplexes containing only G·C base pairs. The quadratic coefficients, $C_i(g)$ and $i = 1$, 2, appeared to be constant within experimental errors and independent of N_{bp} and f(G·C) for our set of 92 DNA duplex oligomers. Therefore, the coefficients $C_i(g)$ were averaged. Parameters evaluated from this analysis were combined into the four T_m salt corrections shown in Table 3. These equations can be used to predict a new melting temperature $T_m(2)$ in buffer of total sodium ion concentration $[Na^+]_2$ if a melting temperature $T_m(1)$ in a reference sodium ion concentration, $[Na^+]_1$, is available either from calculation or direct measurement. In other words, these equations can be used to scale melting temperatures of DNA duplex oligomers to buffers of any sodium ion composition (within the range of sodium ion concentrations studied). Melting temperatures are expressed in kelvins and Na^+ concentration in moles per liter. In the following section, we compare these four new salt corrections with relationships proposed earlier (eqs 7−13) for goodness-of-fit and their accuracy in predicting the melting temperatures of DNA duplex oligomers.

Comparison of New and Previously Published T_m Salt Corrections. The entire melting data set was analyzed statistically. Specifically, all formulas for T_m salt corrections listed in Tables 1 and 3 were used to scale T_m's and compared

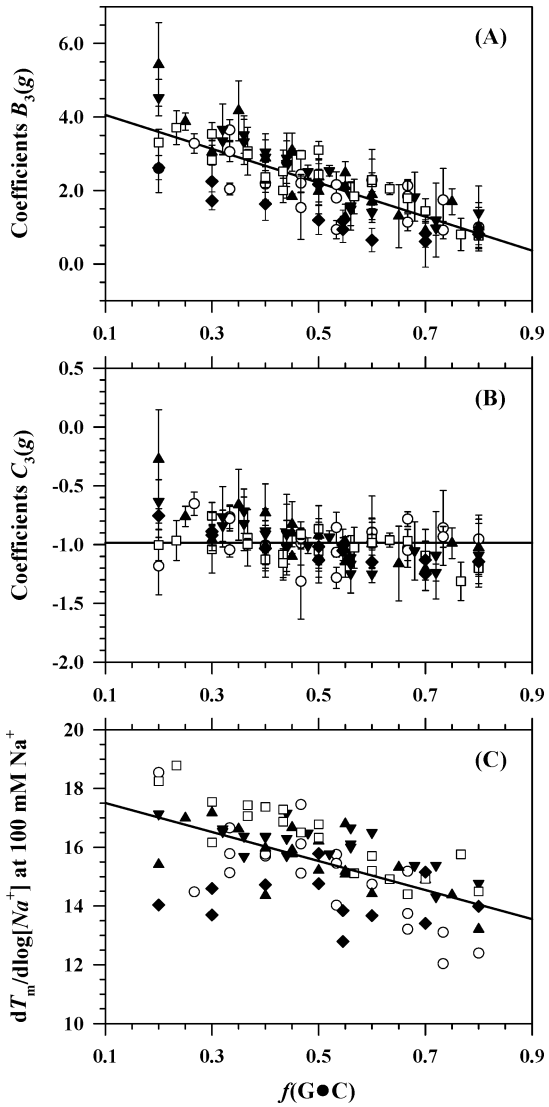

FIGURE 3: Melting temperatures for each of 92 DNA duplex oligomers (g varies from 1 to 92) were fit to the quadratic eq 17. Coefficients obtained from fits, $B_3(g)$ and $C_3(g)$, and values of $dT_m/d \log [Na^+]$ are plotted as a function of f(G·C): (◆) 10 and 11-mers; (○) 15-mers; (▲) 20-mers; (▼) 25-mers; (□) 30-mers.

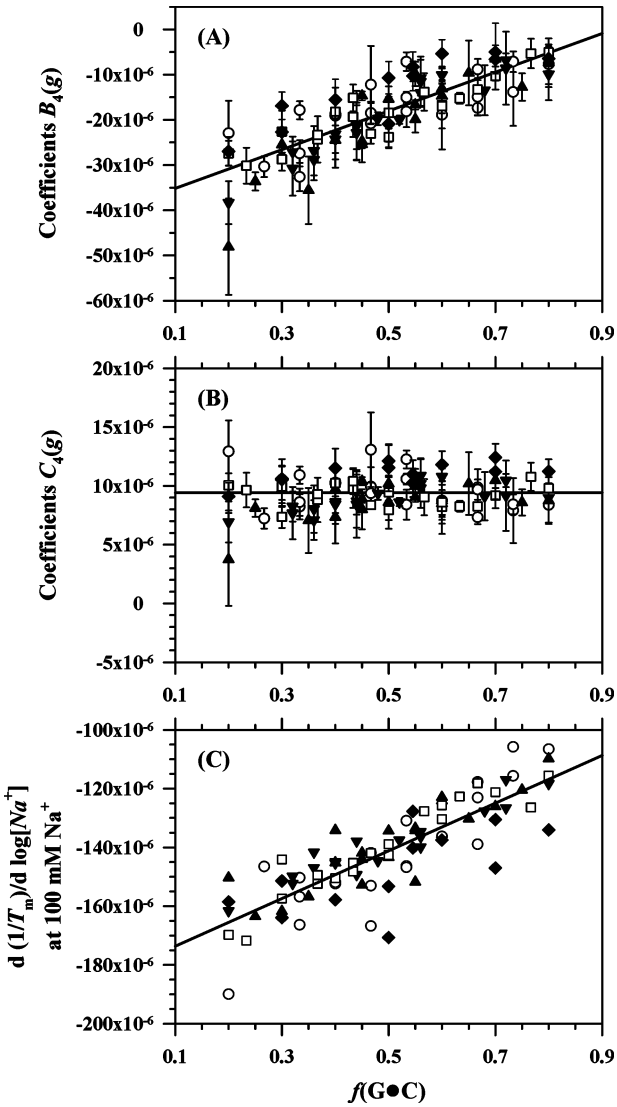

FIGURE 4: Melting temperatures for each of 92 DNA duplex oligomers were fit to the quadratic eq 18. Coefficients obtained from fits, $B_4(g)$ and $C_4(g)$, and values of $d(1/T_m)/d \log [Na^+]$ are plotted as a function of f(G·C): (◆) 10 and 11-mers; (○) 15-mers; (▲) 20-mers; (▼) 25-mers; (□) 30-mers.

as to how well they predict the experimental melting temperatures from Table 2. Because the majority of current nearest-neighbor parameters were determined in 1 M Na^+ (*7*, *11*), this ionic concentration was considered to be the reference condition and was used as the starting point from which all T_m predictions were made. Melting temperatures in 69, 119, 220, and 621 mM Na^+ buffers were calculated using eqs 7−13 and 19−22 for all 92 sequences using our experimentally measured melting temperatures in 1 M Na^+ buffer. Thus, $4 \times 92 = 368$ predicted T_m's for each salt correction formula were obtained. Predicted T_m's were compared with experimentally measured T_m's. Results are summarized in Table 4. Our T_m salt correction (eq 22) predicts T_m's most accurately and has the lowest χ_r^2 values of all the equations considered. Average error of melting temperatures predicted using eq 22 is close to the average experimental error of our T_m measurements. The two $1/T_m$ vs ln [Na^+] functions, eqs 22 and 20, fit the melting data better than the related T_m vs ln [Na^+] functions, eqs 21 and 19. The four newly derived T_m salt corrections, eqs 19−22, all of which include a dependence on f(G·C), fit the experimental data better than any equation that is independent of fraction of G·C base pairs. Furthermore, the two salt correction equations that contain quadratic terms, $\ln^2$ [Na^+], show lower χ_r^2 and $|\langle T_m \rangle|_{AVE}$ values than any of the linear salt corrections, demonstrating the importance of including a quadratic term. Because of the nonlinear dependence of T_m on ln [Na^+], previously published linear salt corrections derived from melting data in low Na^+ concentrations (eqs 7, 8, and 11) show large errors for T_m predictions when scaling from the reference melting temperatures in 1 M Na^+. It is also apparent that salt corrections 12 and 13, derived by SantaLucia et al. using oligomer melting data, perform better than salt corrections that were derived from melting experiments of genomic or plasmid DNAs. This may be a result of deviations from two-state melting behavior, which limit transferability of T_m salt corrections between long DNA polymers and short oligomers.

To rigorously establish statistical significance between the observed χ_r^2 values, we determined the probabilities, P, that

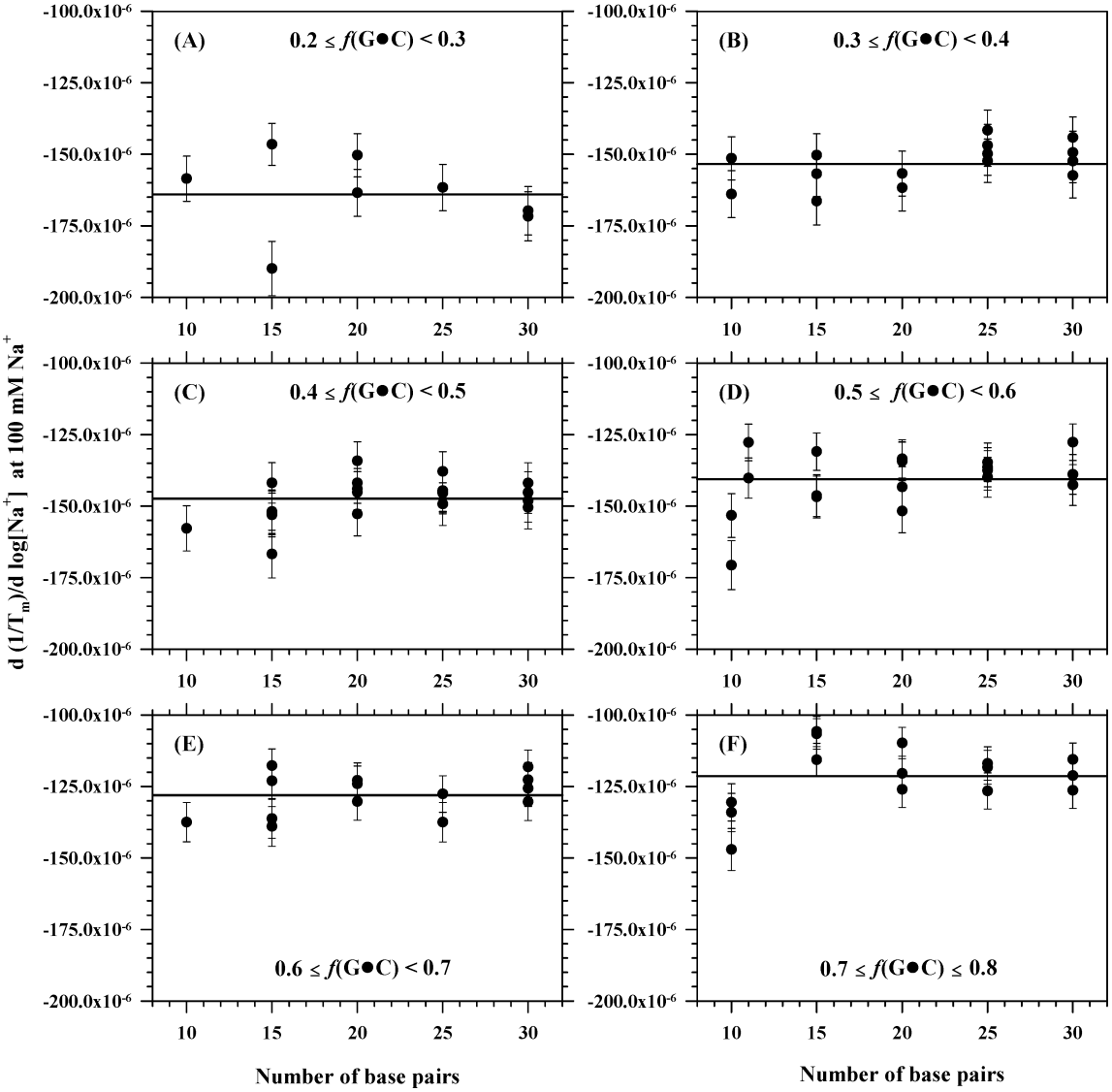

FIGURE 5: Values of $d(1/T_m)/d \log [Na^+]$ from Figure 4C are plotted as a function of oligomer length, N_{bp}. Each graph shows a set of DNA oligomers that have similar f(G·C) within the ranges indicated.

Table 3: New T_m Salt Corrections Derived in This Work for Duplex DNA Oligomers

number	name	equation
19	$T_m - \ln [Na^+]$ equation	$T_m(2) = T_m(1) + (-3.22f(G{\cdot}C) + 6.39) \ln \frac{[Na^+]_2}{[Na^+]_1}$
20	$1/T_m - \ln [Na^+]$ equation	$\frac{1}{T_m(2)} = \frac{1}{T_m(1)} + (3.85f(G{\cdot}C) - 6.18) \times 10^{-5} \ln \frac{[Na^+]_2}{[Na^+]_1}$
21	$T_m - \ln^2 [Na^+]$ equation	$T_m(2) = T_m(1) + (-4.62f(G{\cdot}C) + 4.52) \ln \frac{[Na^+]_2}{[Na^+]_1} - 0.985(\ln^2[Na^+]_2 - \ln^2 [Na^+]_1)$
22	Owczarzy et al. T_m salt correction	$\frac{1}{T_m(2)} = \frac{1}{T_m(1)} + (4.29f(G{\cdot}C) - 3.95) \times 10^{-5} \ln \frac{[Na^+]_2}{[Na^+]_1} + 9.40 \times 10^{-6}(\ln^2 [Na^+]_2 - \ln^2 [Na^+]_1)$

observed differences in χ_r^2 values could happen by random chance alone. The probabilities are summarized in the last column of Table 4. Results reveal that the new T_m salt correction (eq 22) predicts melting temperatures significantly better than any other T_m salt correction formula.

Table 4 lists salt correction equations sorted by accuracy and χ_r^2 values, which were calculated using experimental melting temperatures in a reference ionic environment of 1 M Na^+. Analyses were systematically conducted where the reference ionic environment chosen was one of the lower available sodium ion concentrations (69, 119, 220, or 621 mM Na^+). Melting temperatures were then predicted in the remaining four ionic conditions from the melting temperature obtained in the reference buffer using salt correction eqs 7−13 and 19−22. From the differences between these predicted and experimental melting temperatures, χ_r^2 and $|\langle T_m \rangle|_{AVE}$ values were calculated (data not shown). The salt corrections were again sorted by accuracy. The order of salt

Table 4: Accuracy of Various T_m Salt Corrections Evaluated for Our Data Set of 92 DNA Duplex Oligomers

eq no.	salt correction	χ_r^2	$\lvert\langle T_m\rangle\rvert_{AVE}$ (°C)	P^a
22	Owczarzy et al. T_m salt correction	4.4	0.5	
21	$T_m - \ln^2[Na^+]$ equation	9.9	0.7	2.2×10^{-14}
20	$1/T_m - \ln[Na^+]$ equation	19.5	1.1	2.6×10^{-42}
19	$T_m - \ln[Na^+]$ equation	21.8	1.2	4.5×10^{-48}
13	SantaLucia unified parameters	44.3	1.7	1.0×10^{-89}
12	$T_m - 12.5 \log[Na^+]$ salt correction	68.4	2.1	1.2×10^{-119}
8	Wetmur salt correction	87.3	2.4	6.7×10^{-137}
9	Frank-Kamenetskii equation	175.4	3.7	2.7×10^{-188}
7	Schildkraut−Lifson equation	337.7	5.1	2.0×10^{-238}
10	Marmur−Schildkraut−Doty equation	356.0	5.3	1.9×10^{-242}
11	Blake−Delcourt nearest-neighbor salt correction	372.9	5.3	1.6×10^{-245}

[a] Probabilities that observed differences in values of χ_r^2 for the Owczarzy et al. T_m salt correction and other salt corrections can happen by random chance alone. If these probabilities are less than 0.05, then differences in χ_r^2 are deemed to be statistically significant.

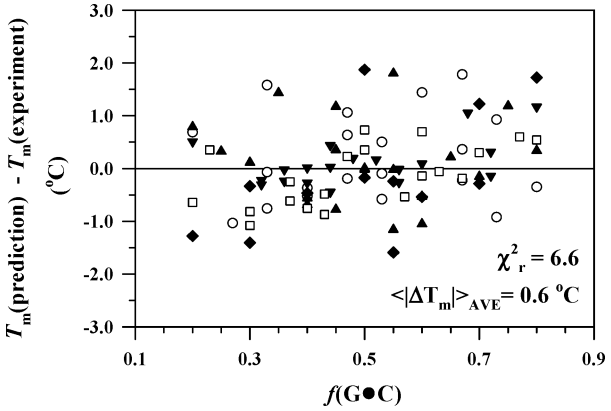

FIGURE 6: Errors of T_m predictions in 69 mM Na^+ scaled from T_m in reference 1 M Na^+ buffer, T_m(prediction) − T_m(experiment), were calculated using salt correction 22 for our UV melting data set of 92 duplex DNAs. The errors are plotted vs f(G•C) for oligomers of various lengths: (◆) 10- and 11-mers; (○) 15-mers; (▲) 20-mers; (▼) 25-mers; (□) 30-mers.

corrections from analyses using each of the four lower sodium ion concentrations as a reference was the same as the order of salt corrections in Table 4.

The above statistical analyses describe the overall accuracy of T_m predictions for the entire 92 duplex data set. Figure 6 graphically demonstrates the accuracy of T_m predictions obtained using salt correction 22 for individual duplexes plotted as a function of f(G•C) in 69 mM Na^+, scaling from the reference 1 M Na^+ buffer so that the largest available range of ionic environments is examined. On average, errors of T_m predictions will be smaller when melting temperatures are predicted over a shorter range of sodium ion concentrations. Figure 6 shows that predicted melting temperatures are within 1.9 °C of experimentally measured values and the average error of T_m predictions is 0.6 °C. Errors of T_m predictions seem to be randomly distributed and did not vary with f(G•C) or N_{bp}.

Figure 7 provides a graphical illustration of the results obtained when different salt correction equations are employed to scale melting temperatures for 2 representative DNA duplex oligomers. The Schildkraut−Lifson eq 7 is

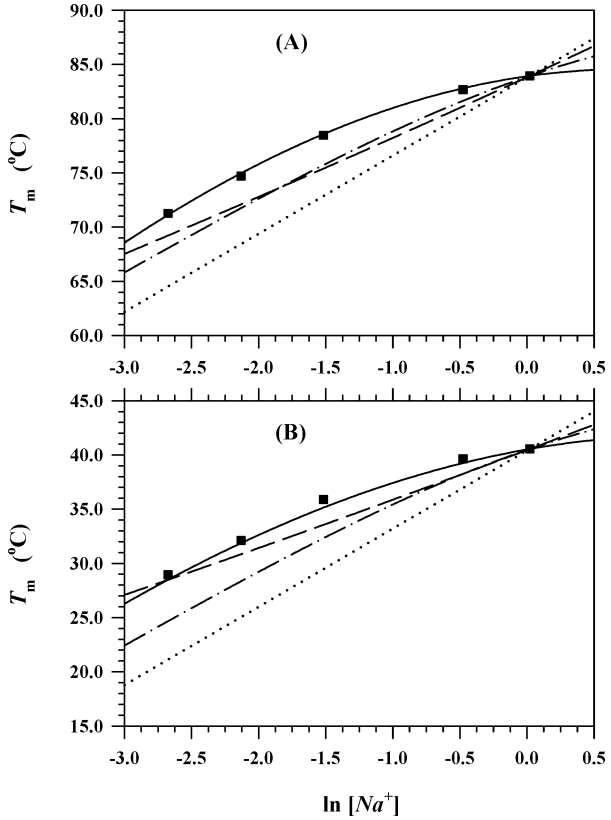

FIGURE 7: Comparison of some commonly used salt corrections and our new T_m salt correction 22. Experimentally measured (■) and predicted melting temperatures for two DNA duplex oligomers from our set, (A) 5′-ACGCCCACAGGATTAGGCTGGCCCA-CATTG-3′ and (B) 5′-CCAACTTCTT-3′, are shown. Salt-corrected melting temperatures from 1 M Na^+ buffer to lower Na^+ concentrations are calculated by Owczarzy et al. T_m salt correction (—), Schildkraut−Lifson equation (•••), Wetmur salt correction (— • —), and SantaLucia unified parameters salt correction (— — —).

particularly prone to error when used to scale melting temperatures from buffers of high ionic concentrations (1 M Na^+), largely due to inaccuracies in the dT_m/d log [Na^+] value. This equation is most accurate when applied within the narrow range of 70−120 mM Na^+, that is, in the range of buffers experimentally used to develop that equation (*1*). At this low ionic concentration, its value of dT_m/d log [Na^+] = 16.0 is similar to the experimentally measured value of dT_m/d log [Na^+] for f(G•C) = 0.4 (see Figure 3c). The Wetmur salt correction [8] offers some improvement over the Schildkraut−Lifson equation, but errors of T_m predictions are still large. Of the previously published methods, the SantaLucia unified parameters salt correction (eq 13) is the most accurate, especially when scaling between 1 M and 70 mM Na^+ buffers. However, this equation predicts melting temperatures less accurately for scaling done between 1 M Na^+ and medium ionic environment (200−600 mM) buffers. This unexpected behavior results from the nonlinear dependence of $1/T_m$ on the logarithm of sodium ion concentration, further reinforcing the importance of the quadratic term in new salt correction equation. As is again demonstrated in Figure 7, melting temperatures predicted using our new T_m salt correction (eq 22) show the smallest deviations from experimental melting temperatures over the full range of tested ionic environments.

It is expected that equations derived using a particular data set will accurately predict results for that same data set. A better test of the validity and utility of the new equations can be obtained if these equations are used to scale T_m's for an independent data set.

Evaluation of T_m Salt Corrections Based on an Independent Validation Data Set of T_m Measurements. Equations 7−13 and 19−22 were used to predict melting temperatures for a validation set of duplex DNA oligomers that were not used to fit coefficients in eqs 19−22, and the predicted T_m's were compared with measured melting temperatures. A collection of 60 pairs of T_m measurements in monovalent ion buffers of different ionic concentrations were obtained from the published literature, as well as the Thermodynamic Database of Nucleic Acids (*64*). DNA concentrations were the same for each pair of T_m measurements but did vary between studies. The independent validation data set consists of 48 unique sequences ranging in length from 6 to 30 base pairs and is listed in Table 5. The reported melting temperature obtained from buffer of higher sodium ion concentration was used as reference point for each T_m pair, and the various salt correction equations were applied to predict the T_m under lower sodium ion concentrations. Predicted T_m's were then compared with experimentally measured melting temperatures. Using eqs 3 and 4 and $\sigma_{T_m} = 0.75$ °C, which was the average error reported for the validation data set, we calculated values of χ_r^2 and $|\langle T_m \rangle|_{AVE}$ for each T_m salt correction, and they are shown in Table 6.

The rank order of accuracy for each of the salt correction equations was similar for the validation data set as for our data set of 92 duplex DNAs (compare trends in Tables 4 and 6). Again, our new T_m salt correction (eq 22) resulted in the lowest average error of T_m predictions (±1.6 °C) and the lowest χ_r^2 value. Hence we conclude that this equation is currently the most accurate formula to scale T_m between environments of different monovalent cation concentrations. As an added level of comparison, pairwise probabilities that the observed differences in χ_r^2 could happen by random chance alone were calculated and are shown in the last column of Table 6. The T_m salt correction 22 is significantly more accurate than any previously published salt correction equation. Although the new T_m−ln^2 [Na$^+$] salt correction (eq 21) results in higher χ_r^2 values than eq 22, it is not statistically different from T_m salt correction 22 for the validation data set, $P = 0.17$.

Not surprisingly, the average errors of T_m predictions were higher for the validation data set (obtained from a variety of sources) than the errors observed for predictions within our set of 92 duplex DNAs. This might result from the higher experimental errors for melting temperatures in the validation data set, which were typically reported to be in the range of 0.5−1.0 °C, in comparison with the experimental errors for the melting temperatures measured in our experiments, which were about 0.3 °C. Lower accuracy of the validation set will lead to higher values of $|\langle T_m \rangle|_{AVE}$ since average deviations between predicted and experimental melting temperatures cannot be smaller than experimental T_m errors. The values of χ_r^2 are also higher for the validation set because χ_r^2 is a function of both the accuracy of the model and the accuracy of data studied. Adding further uncertainty to interpretation, the duplex DNA oligomers studied in the validation set were purified by a variety of techniques, and in no case was the sample purity assessed quantitatively.

Expansion of T_m Salt Correction to Include Nearest-Neighbor Parameters. The T_m salt correction 22 can be expanded to include sequence-specific nearest-neighbor interactions (*9*, *73*, *74*). Sequence-dependent nearest-neighbor parameters, $(B_4)_{ij}^{n-n}$ and $(C_4)_{ij}^{n-n}$, were derived from the coefficients $B_4(g)$ and $C_4(g)$ of eq 18 using an approach described in the Supporting Information. The resulting parameters were used in the following nearest-neighbor salt correction function:

$$\frac{1}{T_m(2)} = \frac{1}{T_m(1)} + \sum_{ij=A,T,C,G,E} ((B_4)_{ij}^{n-n} f_{ij}) \ln \frac{[Na^+]_2}{[Na^+]_1} + \sum_{ij=A,T,C,G,E} ((C_4)_{ij}^{n-n} f_{ij})(\ln^2 [Na^+]_2 - \ln^2 [Na^+]_1) \quad (23)$$

where f_{ij} is the fraction of occurrence for the particular nearest-neighbor doublet in the duplex sequence and sums are calculated over all 12 unique nearest-neighbor doublets (*74*) including ends (E).

This nearest-neighbor version of our quadratic salt correction equation (eq 23) was used to predict melting temperatures in 69, 119, 220, and 621 mM Na$^+$ buffers starting from measured melting temperatures in reference 1 M Na$^+$ buffer for the entire set of 92 sequences. From predicted T_m's and formulas 3 and 4, values of $\chi_r^2 = 2.8$ and $|\langle T_m \rangle|_{AVE} = 0.4$ °C were obtained for salt correction function 23 and were compared to the statistical values for eq 22 shown in Table 4. Very little improvement in the accuracy of T_m prediction is seen between the nearest-neighbor function 23 and the original T_m salt correction 22, while the number of fitted parameters increases from three for T_m salt correction 22 to 24 parameters for the nearest-neighbor salt correction 23. The nearest-neighbor salt correction 23 was also used to predict melting temperatures for the validation data set (Table 5). When compared with measured melting temperatures, values of $\chi_r^2 = 19.1$ and $|\langle T_m \rangle|_{AVE} = 1.7$ °C were calculated. Surprisingly, inclusion of nearest-neighbor terms in the salt correction equation did not improve χ_r^2 and $|\langle T_m \rangle|_{AVE}$ values and resulted in less accurate predictions than original salt correction equation 22 (Table 6). Although the relationship between cation concentration and the T_m of duplex DNA oligomers is sequence-dependent, this effect seems to be sufficiently modeled by a simple relationship with f(G·C) term rather than a more complex equation (eq 23) that includes nearest-neighbor parameters in the analysis. Thus only three parameters are needed in T_m salt correction function 22 to scale melting temperatures between environments of different monovalent ion concentration within the experimental errors.

It is important to define the functional limits that apply to use of eq 22, particularly the range of oligomer length, range of oligomer concentration, and range of buffer Na$^+$ concentration that can be employed and maintain reasonable accuracy. Equation 22 was derived using T_m data for oligomers ranging in length from 10 to 30 base pairs in buffers ranging from 69 mM to 1.0 M Na$^+$ at an oligomer concentration of 2 μM. We have already demonstrated its accuracy under these conditions.

Table 5: Independent Validation Set of 60 T_m Pairs for 48 DNA Duplex Oligomers Compiled from Published Sources[a]

sequence (5′ to 3′)	ref	C_t (μM)[b]	$[Na^+]_1$ (mM)[c]	exptl $T_m(1)$ (°C)[d]	$[Na^+]_2$ (mM)[c]	exptl $T_m(2)$ (°C)[d]	predicted $T_m(2)$ (°C) by salt correction		
							eq 22[e]	eq 13[f]	eq 7[g]
ACCGCA	*29*	8.0	1015	27.9	415	26.2	26.4	24.3	21.5
ACCGCA	*29*	8.0	615	27.5	165	24.7	23.7	22.2	18.0
GCATGC	*28*	100.0	1000	38.3	42	29.2	26.3	25.8	15.4
GCATGC	*28*	100.0	1000	38.3	150	35.5	33.1	30.7	24.6
CCAAACA	*65*	30.0	1015	35.0	115	21.0	26.7	25.5	19.3
TTGCGCAA	*67*	1.1	1015	40.8	165	35.4	34.7	33.1	27.7
GGAATTCC	*30*	8.5	1015	33.0	115	24.5	25.4	23.8	17.3
GGAATTCC	*31*	18.8	1000	37.1	200	30.0	32.0	30.0	25.5
GGAATTCC	*31*	18.8	400	33.2	100	24.5	27.0	27.2	23.2
GGAATTCC	*30*	170.0	1015	43.5	115	34.5	35.4	33.6	27.8
GGAATTCC	*66*	3000.0	267	50.0	92	42.0	44.2	44.9	42.3
GCCAGTTAA	*29*	8.0	1015	38.0	265	34.2	33.8	32.1	28.3
GCCAGTTAA	*29*	8.0	415	36.1	115	30.0	30.2	30.5	26.8
GGATGGGAG	*33*	5.2	1010	43.6	155	39.2	38.4	35.1	30.1
AAAAAAAAAA	*34*	6.4	1010	32.0	160	24.0	22.6	23.7	18.7
AAAAAAAGTT	*8*	3.5	1000	32.4	115	22.4	21.6	22.7	16.8
TGAAAAAAAA	*8*	8.0	1000	32.9	115	21.3	22.0	23.3	17.3
CATATATATG	*8*	17.9	1000	32.5	115	24.8	22.5	22.9	16.9
GTAGTAGTAG	*8*	3.6	1000	36.9	115	29.6	28.2	27.3	21.3
TTAATAGGGG	*8*	7.2	1000	40.0	115	30.9	31.2	29.8	24.4
GTAGATCACT	*35*	7.2	515	43.0	65	31.0	32.2	33.4	28.1
GTAGATCACT	*68*	10.0	515	43.7	115	36.3	36.5	36.7	32.9
ATTATGGGGC	*8*	5.4	1000	44.7	115	37.5	36.5	34.6	29.1
ACAGTGACAC	*8*	8.9	1000	50.5	115	43.8	42.0	40.5	34.9
GACGTGTGAC	*8*	35.6	1000	55.7	115	48.8	48.0	46.0	40.1
ATATAGCTATAT	*8*	1.7	1000	37.1	115	27.3	26.5	26.7	21.5
CAAAGATTCCTC	*36*	5.0	210	44.8	98	40.3	40.4	41.3	39.3
CAAAGATTCCTC	*36*	5.0	210	44.8	21	29.3	28.9	34.5	28.3
CTTTCTCTCCCT	*69*	5.0	1015	53.3	65	39.4	41.0	40.0	33.5
CGCGAATTCGCG	*37*	18.1	1001	66.4	101	56.1	58.0	56.2	49.9
CGCGAATTCGCG	*37*	18.1	1001	66.4	11	37.5	40.9	46.9	34.0
CCGGCCGCGCGC	*70*	5.0	1015	76.8	115	72.3	72.4	66.8	61.1
TAATTAATTAATTA	*38*	0.7	1020	38.3	220	29.8	30.5	30.8	27.2
TAATTAATTAATTA	*38*	5.0	800	42.0	400	38.6	38.6	38.5	37.0
AAATATAGCTATATTT	*8*	1.2	1000	48.7	115	36.7	36.9	37.8	33.1
ATATATAGCTATATAT	*8*	1.2	1000	45.5	115	35.5	34.0	45.5	45.5
AAAAAAAGCTTTTTTT	*8*	1.5	1000	53.3	115	41.0	41.2	42.7	37.7
AACGTGAATTCTGGCA	*8*	6.9	1000	67.9	115	58.4	57.9	56.8	52.3
CGCGCGCGACTGACTG	*32*	5.5	115	69.4	15	56.1	54.1	60.1	54.7
AATATATGAATTCTAATTAA	*8*	0.9	1000	53.4	115	41.0	41.1	42.3	37.8
ATATATATAGCTATATATAT	*8*	1.1	1000	53.0	115	42.4	40.7	41.6	37.4
AAAAAAAAAGCTTTTTTTTT	*8*	1.6	1000	58.8	115	49.2	46.1	47.9	43.2
AAATAAATAGCTATTTATTT	*8*	2.5	1000	58.4	115	44.8	45.7	47.1	42.8
AACGCGTGAATTCTGGCCAA	*8*	5.1	1000	75.3	115	66.4	65.5	64.0	59.7
GCTAAAAAGAGAGAGAGATCG	*71*	3.2	1015	69.0	215	61.0	62.7	61.0	57.8
AATATATATAGAGTAATTATAA	*8*	0.9	1000	54.8	115	42.6	42.3	43.4	39.2
AAATATAAGAATTCTTATATTT	*8*	0.9	1000	56.9	115	46.3	44.2	45.6	41.3
ATATATATGAATTCATATATAT	*8*	1.2	1000	56.4	115	48.2	43.8	44.9	40.8
ATAAAAATGAATTCATTTTTAT	*8*	1.8	1000	61.3	115	51.2	48.3	49.9	45.7
AAAAAAAAGAATTCTTTTTTTT	*8*	2.0	1000	61.3	115	49.6	48.3	50.1	45.7
AATATATATAGAGTGGCCGCAA	*8*	1.0	1000	70.0	115	63.2	59.1	58.4	54.4
AATATATATAGAGTGCGCGCAA	*8*	1.1	1000	69.2	115	62.9	58.3	58.0	53.6
AACGCGCGTAGAGTAATTATAA	*8*	1.2	1000	67.1	115	62.9	56.4	56.1	51.5
AACGCCGGTAGAGTGCGCGCAA	*8*	1.1	1000	81.8	115	77.4	73.2	70.6	66.2
AACGCGCGTAGAGTGGCCGCAA	*8*	1.6	1000	82.6	115	75.5	73.9	71.3	67.0
AACGCGCGTGAATTCTGGCCGCAA	*8*	2.3	1000	81.7	115	74.6	72.5	70.4	66.1
AAAAAAAAAAAAAAAAAAAAAAAAAA	*72*	2.0	810	62.0	210	53.0	53.7	54.9	52.3
AAAAAAAAAAAAAAAAAAAAAAAAAA	*72*	2.0	410	58.0	110	48.0	48.4	51.3	48.5
$(CAG)_{10}$	*24*	3.3	167	83.0	19	67.0	65.9	71.7	67.3
$(GAC)_{10}$	*24*	3.3	167	83.0	19	66.0	65.9	72.1	67.3

[a] None of these melting temperatures were used to derive our new T_m salt corrections, that is, eqs 19−22. [b] Melting experiments in both ionic environments were conducted at this identical total single-strand DNA concentration. [c] Total sodium ion concentrations included contributions from buffer salts. [d] $T_m(1)$ and $T_m(2)$ are experimental melting temperatures observed in buffers of $[Na^+]_1$ and $[Na^+]_2$, respectively. [e] Owczarzy et al. T_m salt correction. [f] SantaLucia unified parameters equation. [g] Schildkraut−Lifson equation.

Oligomer Length. Table 5 includes seven sequences with reported T_m data from the published literature that are shorter than 10 base pairs, including duplexes of 6, 7, 8, and 9 bp length (see rows 1−14). When experimental T_m for these short oligomers are compared with scaled melting temperatures predicted using eq 22, we find an average error of $|\langle T_m \rangle|_{AVE} = 1.6$ °C with $\chi_r^2 = 10.7$, values that are nearly identical to results obtained when all 48 published duplexes

Table 6: Accuracy of Various T_m Salt Corrections Evaluated for the Validation Set of 48 DNA Duplex Oligomers

eq no.	salt correction	χ_r^2	$\lvert\langle T_m\rangle\rvert_{AVE}$ (°C)	P^a
22	Owczarzy et al. T_m salt correction	8.4	1.6	
21	$T_m - \ln^2[Na^+]$ equation	12.1	2.0	0.17
20	$1/T_m - \ln[Na^+]$ equation	19.7	2.4	1.5×10^{-03}
19	$T_m - \ln[Na^+]$ equation	24.1	2.9	1.0×10^{-04}
13	SantaLucia unified parameters	26.5	2.6	4.5×10^{-05}
12	$T_m - 12.5 \log[Na^+]$ salt correction	26.3	3.0	2.6×10^{-05}
8	Wetmur salt correction	28.9	3.1	5.9×10^{-06}
9	Frank-Kamenetskii equation	54.4	4.8	3.9×10^{-11}
7	Schildkraut−Lifson equation	73.1	5.5	5.2×10^{-14}
10	Marmur−Schildkraut−Doty equation	90.2	6.3	4.2×10^{-16}
11	Blake−Delcourt nearest-neighbor salt correction	106.9	6.4	1.9×10^{-17}

[a] Probabilities that differences in values of χ_r^2 for the Owczarzy et al. T_m salt correction and other salt corrections can happen by random chance alone.

are considered. Similar analysis of 6−9 bp oligomers carried out using Schildkraut−Lifson eq 7 and SantaLucia universal parameters salt correction 13 yields average errors of 6.0 and 2.4 °C, respectively. Within our own data set, predictions for short oligomers are slightly less accurate than those for longer oligomers (Table S-3 of Supporting Information). Nevertheless, even for the shortest lengths examined eq 22 remains significantly more accurate than other published methods of scaling T_m.

Six DNA duplexes of 40−60 base pairs in length with G·C base pair content ranging from 30% to 70% were studied to test whether eq 22 could be applied to longer DNAs. Results of UV melting experiments are summarized in Table 7. Although these longer DNA duplex oligomers show a single melting transition, their melting curves are slightly asymmetric (Figure 1), which suggests that there may be some departure from the simple two-state melting behavior. Nevertheless, transitions were sharp such that T_m could readily be determined. Both denaturation and annealing melting curves overlapped, and experimental melting temperatures were reproducible within 0.3 °C. Various ionic environments were used as a reference buffer in Table 7 to investigate accuracy of salt corrections to scale T_m over the different ranges of sodium ion concentrations. The T_m salt correction eq 22 is still accurate in scaling T_m between ionic environments for these longer DNAs. Melting temperatures predicted using eq 22 are reported in column 6 of Table 7 and deviate on average by only 0.3 °C from experimentally measured melting temperatures, which is within the limits of experimental error. In comparison, the SantaLucia unified parameter salt correction 13 and the Schildkraut−Lifson eq 7 exhibit average errors of 1.4 and 2.6 °C, respectively. We therefore have evidence for a length range of at least 6−60 base pair duplex where eq 22 can be employed.

Examination of T_m Salt Corrections at Various DNA Concentrations. The UV melting experiments reported in Table 2 were conducted using a total single-strand DNA concentration of 2 μM. To further test the utility of eq 22, melting studies were performed with 90-fold higher DNA concentrations using differential scanning calorimetry for a subset of 81 DNA duplexes in 69 mM and 1 M Na^+ buffers (see Materials and Methods). A resulting data set of 162 experimental calorimetric T_m measurements is presented in Table S-2 of Supporting Information.

Melting temperatures obtained from calorimetric measurements in 1 M Na^+ were used to predict melting temperatures in 69 mM Na^+ buffer, and predictions were compared with experimentally measured T_m's. Using eqs 3 and 4 and the observed error $\sigma_{T_m} = 0.3$ °C for the calorimetric measurements, we obtained statistical values of $\chi_r^2 = 4.7$ and $\lvert\langle T_m\rangle\rvert_{AVE} = 0.5$ °C when eq 22 was applied to the DSC experimental data set, similar to the χ_r^2 value of 6.6 and $\lvert\langle T_m\rangle\rvert_{AVE} = 0.6$ °C calculated from UV optical melting data set (Figure 6). An *F*-test shows no significant difference between χ_r^2 obtained at these two different DNA concentrations ($P = 0.13$). The errors of T_m predictions are shown in Figure 8 and appear to be insensitive to both N_{bp} and f(G·C). Our new T_m salt correction therefore can be used to scale T_m's of duplex DNAs at high DNA concentrations ($C_t = 180$ μM) with similar accuracy to low DNA concentrations ($C_t = 2$ μM); the utility of eq 22 is not limited to the DNA concentrations of our optical melting studies.

Accuracy at Low Sodium Ion Concentrations. It is of little practical value to examine the accuracy of eq 22 above 1 M Na^+. However, the utility of this equation as Na^+ concentration decreases below 69 mM is interesting to consider, particularly with respect to counterion condensation theory, which predicts a strictly linear relationship between Na^+ concentration and T_m below 100 mM Na^+ (*75*, *76*, *94*). Experimental T_m results have been previously reported for

Table 7: Experimental and Predicted Melting Temperatures for 40 and 60 Base Pair Long DNA Duplex Oligomers[a]

sequence (5′ to 3′)	$[Na^+]_1$ (mM)	exptl $T_m(1)$ (°C)[b]	$[Na^+]_2$ (mM)	exptl $T_m(2)$ (°C)[b]	predicted $T_m(2)$ (°C) by salt correction: eq 22[c]	eq 13[d]	eq 7[e]
GCAATAGAAAGAGGAAATAATAGTTTTATATTCGACCTAG	1021	75.4	220	68.0	68.0	66.9	64.3
AGCTGACGCCAAGTCCAAATCTAACCACATGCAAGACACG	1021	84.5	119	74.5	74.4	72.7	69.0
GTCCGCATCCCGAGAGCCATGTGGTGACCCTGCGCCGCAC	69	78.7	621	90.1	89.7	90.7	94.5
GAATATACCCAGAAGAATTGGTTTGACAGGTTAATTAGAA-TATTTAGTCTGATACAATTG	621	78.4	119	68.2	68.3	69.1	66.5
CGGAGAGGGACAGCTAGTGCCCCTGTGGGGAGTCGCTTAT-ACAAAGCGGAGTGCAATTTT	69	75.2	220	83.5	83.1	81.6	83.5
GGCACACGCCATGCGGCTTCCAGGCTTGGACGGACCTGCC-CTTGGAACCGGTCGGGACGC	220	87.7	69	79.5	80.5	81.4	79.4

[a] Melting experiments in both ionic environments are conducted at 2 μM total single-strand DNA concentrations. [b] $T_m(1)$ and $T_m(2)$ are melting temperatures observed in buffers of $[Na^+]_1$ and $[Na^+]_2$, respectively. [c] Owczarzy et al. T_m salt correction. [d] SantaLucia unified parameters equation. [e] Schildkraut−Lifson equation.

eight duplexes that include measurements conducted in Na^+ concentration below 69 mM (Table 5, rows 3, 21, 28, 29, 31, 39, 59, and 60). For this subset of oligomers, the Na^+ concentration studied ranged from 11 to 65 mM. The accuracy of eq 22 when applied to low-salt conditions was tested by comparing predicted (scaled) T_m with experimental T_m for these duplexes. Statistical analysis showed that eq 22 continues to be accurate to scale T_m even into this low-salt range with $|\langle T_m \rangle|_{AVE} = 1.6$ °C and $\chi_r^2 = 10.6$. While a precise lower limit for Na^+ concentration cannot be defined from these data to set boundaries wherein eq 22 can be applied, it does appear that the equation can be employed to accurately scale T_m for sodium ion concentrations substantially below 69 mM, the lowest concentration in the set of experimental data used in the derivation of eq 22. Additional experiments to study melting behavior of our oligomer set in low sodium ion concentrations are ongoing.

Specific Example of Calculations Using New T_m Salt Correction 22. Use of our new T_m salt correction formula 22 is illustrated with an example calculation where T_m is scaled from a known reference point (in this case a measured melting temperature obtained in 621 mM Na^+ buffer) to a new T_m in 1×SSC buffer, which contains 150 mM Na^+. The example sequence is a 20 base pair duplex with eight G·C base pairs, 5′-ATGCAATGCTACATATTCGC-3′. The reference T_m was obtained at 2 μM single-strand concentration. This duplex has a melting temperature of 67.0 °C in 621 mM Na^+ melting buffer, T_m(621 mM). The duplex mole fraction of G·C base pairs is

$$f(\text{G·C}) = \frac{N_{\text{G·C}}}{N_{\text{bp}}} = \frac{8}{20} = 0.400$$

Equation 22 is then applied to estimate a melting temperature at 150 mM Na^+, T_m(150 mM),

$$\frac{1}{T_m(150\text{ mM})} = \frac{1}{T_m(621\text{ mM})} + (4.29f(\text{G·C}) - 3.95) \times 10^{-5} \ln\frac{[Na^+]_2}{[Na^+]_1} + 9.40 \times 10^{-6}(\ln^2[Na^+]_2 - \ln^2[Na^+]_1)$$

$$= \frac{1}{67.0 + 273.15} + (4.29 \times 0.400 - 3.95) \times 10^{-5} \ln\frac{0.150}{0.621} + 9.40 \times 10^{-6}(\ln^2 0.150 - \ln^2 0.621)$$

$$= 3.0033 \times 10^{-3}\ \text{K}^{-1}$$

with the result that T_m(150 mM) = 333.0 K = 59.8 °C.

THEORETICAL DISCUSSION

The improved eq 22 to scale or correct T_m as a function of monovalent cation concentration presented in this work was derived in an entirely empirical fashion. We will more fully consider the theoretical thermodynamic implications of the observed quadratic equation later (Owczarzy et al., manuscript in preparation). We suggest here plausible hypotheses for our observations.

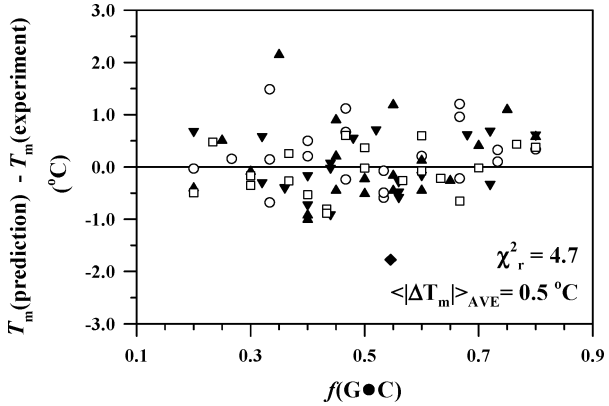

FIGURE 8: Confirmation of our new T_m salt correction 22 using DSC melting experiments. From experimentally measured calorimetric melting temperatures in reference 1 M Na^+ buffer, melting temperatures were predicted in 69 mM Na^+ buffer and compared with experimental ones. Errors of predictions in 69 mM Na^+ buffer, T_m(prediction) − T_m(experiment), are plotted vs fraction of G·C base pairs for oligomers of various lengths: (◆) 11-mer; (○) 15-mers; (▲) 20-mers; (▼) 25-mers; (□) 30-mers.

Equilibrium between the single-stranded oligomers (S_1, S_2) and the duplex (D) can be shown schematically as

$$S_1\cdot(Na^+)_{n_1} + S_2\cdot(Na^+)_{n_2} + \Delta n Na^+ \leftrightarrows D\cdot(Na^+)_{n_1+n_2+\Delta n} \quad (24)$$

Sodium ions bind to DNA in both the duplex and single-strand states but to a greater degree in the duplex form. Hybridization of two single strands is thus accompanied by a net uptake of Δn sodium ions from solution, that is, a positive Δn value is obtained for duplex formation. As pointed by Laing et al. (*92*), if the sodium ion concentration is sufficiently large and sodium ions saturate binding sites in both the single-stranded and double-stranded states, the value of Δn will indicate the difference in the number of ion binding sites between these states. Counterion uptake during duplex formation is predicted by the counterion condensation theory of charged linear polyelectrolytes (*75*−*78*, *93*, *94*) and is supported by experimental evidence from ^{23}Na-NMR studies (*79*), conductivity and sodium ion activity measurements (*80*, *81*), and recent calorimetric studies (*82*). Assuming a two-state melting transition between the single strands and the duplex, it was shown (*76*, *92*) that the effect of sodium ion concentration on the melting temperature is given by

$$\frac{dT_m}{d\ln[Na^+]} = \frac{-\alpha R T_m^2}{\Delta H^\circ}\Delta n \quad (25)$$

or equivalently in terms of the reciprocal melting temperature

$$\frac{d\left(\frac{1}{T_m}\right)}{d\ln[Na^+]} = \frac{\alpha R}{\Delta H^\circ}\Delta n \quad (26)$$

where ΔH° is the enthalpy of association of DNA from the melted coil to the duplex, R is the ideal gas constant, and α is a correction term for the sodium ion activity coefficient (*29*, *76*) and is about 0.92 at 100 mM Na^+. Laing et al. (*92*) derived eq 26 from sets of coupled multiple binding equilibria

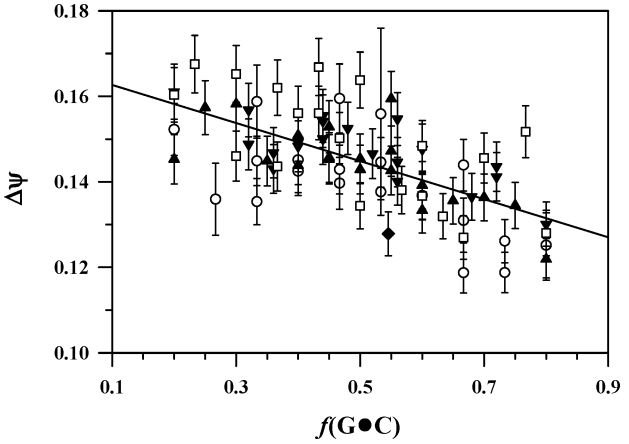

FIGURE 9: Differential ion association parameters, $\Delta\psi$, calculated in 100 mM Na^+ plotted vs fraction of G·C base pairs for oligomers of various lengths: (◆) 11-mer; (○) 15-mers; (▲) 20-mers; (▼) 25-mers; (□) 30-mers.

and suggested a method to distinguish between nonspecific and site-specific ion binding.

Equation 25 was used as the theoretical starting point when empirically deriving new eqns 19 and 21. Equation 26 was used as the theoretical starting point for the new eqs 20 and 22. We therefore fit both T_m and $1/T_m$ as a function of ln [Na^+]. Comparing eqs 19 with 20 and 21 with 22, use of $1/T_m$ always resulted in a better fit than T_m vs ln [Na^+], as shown in Tables 4 and 6. The observed differences in goodness-of-fit are small, however, as would be expected within the narrow range of T_m's (in Kelvin) between 69 mM and 1 M Na^+ buffers for any given oligomer.

Equation 26 suggests that the empirical coefficients in the new T_m salt correction eq 22 depend largely on the ratio of Δn and $\Delta H°$. In the counterion condensation theory of Record and Manning (*75*−*77*, *94*), the sodium ions associated per phosphate group in the DNA duplex and the two single strands are designated ψ_h, $\psi_{c,1}$, and $\psi_{c,2}$, respectively. Therefore, the net sodium ion uptake is

$$\Delta n = 2(N_{bp} - 1)\left(\psi_h - \frac{\psi_{c,1} + \psi_{c,2}}{2}\right) = 2(N_{bp} - 1)\Delta\psi \quad (27)$$

where $2(N_{bp} - 1)$ is the number of phosphate groups in the DNA duplex. Combining eqs 26 and 27 yields

$$\Delta\psi = \frac{d\left(\frac{1}{T_m}\right)}{d \ln [Na^+]} \frac{\Delta H°}{2(N_{bp} - 1)\alpha R} \quad (28)$$

Figure 4c demonstrates that values of $d(1/T_m)/d \ln [Na^+]$ are negative and sequence-dependent and decrease in absolute value with increasing f(G·C) of the oligomer. The values of $\Delta H°/(2(N_{bp} - 1))$ are negative and increase in absolute value as f(G·C) is increased. Values of ΔH_{DSC} were measured in DSC experiments for 81 duplexes in 69 mM and 1 M Na^+ buffers. The observed values of ΔH_{DSC} per mole of duplex varied little with Na^+ concentration and DNA concentration (manuscript in preparation). Therefore the values of ΔH_{DSC} were used to calculate $\Delta\psi$ from eq 28. Figure 9 shows the dependence of $\Delta\psi$ on oligomer G·C base pair content at 100 mM Na^+. Values of $\Delta\psi$ decrease with increasing fraction of G·C base pairs. In principle, it is possible that $\Delta\psi$ may actually be dependent on the fraction of nearest-neighbor doublets, since the $\Delta H°/(2(N_{bp} - 1))$ term of eq 28 can vary because of nearest-neighbor interactions even for duplexes of the same f(G·C). However, these nearest-neighbor effects are smaller than the experimental errors of $d(1/T_m)/d \ln [Na^+]$ and $\Delta\psi$. Therefore, we conclude that, in the first approximation, the values of $\Delta\psi$ decrease with increasing fraction of G·C base pairs. In other words, G·C-rich oligomers bind fewer additional sodium ions upon duplex formation than do A·T-rich oligomers.

According to counterion condensation theory, binding of sodium ions by both duplex and single strands is primarily determined by the negative linear charge density of the oligomer (*75*, *76*, *93*, *94*) and, for concentrations at least up to 100 mM Na^+, is independent of sodium ion concentration. Counterion condensation theory predicts $\psi_h = 0.88$ and $\psi_c = 0.71$. Thus $\Delta\psi = 0.17$. Interestingly, this value of $\Delta\psi$ is what would be predicted for 100% A·T oligomers from the data in Figure 9. Linear least-squares fit of the data in Figure 9 yields the following equation (for 0.1 M Na^+):

$$\Delta\psi = 0.17 - 0.044f(G·C) \quad (29)$$

Equation 29 indicates that $\Delta\psi$ decreases as oligomer f(G·C) increases. Our results are in surprisingly good agreement with the dependence of $\Delta\psi$ on f(G·C) obtained from high-resolution melting data of long λ DNA fragments (see Figure 10 in ref *14*), where least-squares fit resulted in a similar relationship (for 0.14 M Na^+),

$$\Delta\psi = 0.17 - 0.060f(G·C) \quad (30)$$

The observation that $\Delta\psi$ decreases as f(G·C) increases could be explained if high f(G·C) oligomers bind fewer sodium ions in the duplex state than low f(G·C) oligomers or, more likely, if there is increased sodium ion binding by high f(G·C) oligomers in the single-stranded state. Blake and Haydock suggest that Na^+ binding to single-stranded DNA is increased for sequences of higher G·C content, perhaps because of a more collapsed structure and hence increased negative charge density of G·C-rich sequences (*14*).

Counterion condensation models and simulations for DNA duplexes suggest that fewer cations bind near the ends of the oligomer than in the interior (*75*, *76*, *83*, *84*, *94*). This end-region domain is assumed to be of similar length for all oligomers. Consequently, values of $\Delta\psi$ and the corresponding effects of salt on oligomer melting temperatures are thought to increase with oligomer length (*39*, *75*, *76*). On the basis of the experimental data for a set of $d(TA)_n$ hairpins (*23*), it was suggested (*75*, *76*, *94*) that values of $\Delta\psi$ vary linearly with $1/N_{bp}$. In contrast, we find that the dependence of $\Delta\psi$ on f(G·C) is unaffected by oligomer length within the range of 10 to 30 base pairs. This observation, however, can still be consistent with lower sodium ion binding at the ends of oligomers since values of $\Delta\psi$ relate to *differences* between cation binding to the duplex and to the melted single strands. If cation binding in the end region is similarly reduced for both the duplex and single strands, then $\Delta\psi$ will have similar values for both interior and end regions of the oligomer and would appear to be independent of oligomer lengths.

For ease of use, we derived the new T_m salt correction 22 as a function of sodium ion concentration. To examine whether consideration of sodium ion activities is responsible for the nonlinear nature of the plots shown in Figure 2, we estimated average ion activity coefficients using published methods (*85*) and generated new plots of $1/T_m$ vs ln a_{Na^+} for our set of 92 duplex DNAs (data not shown). These plots are still nonlinear and exhibit similar curvature trends as do plots of $1/T_m$ vs ln [Na^+] over the studied range of sodium ion concentrations. Therefore changes in the activity coefficient of sodium ions do not explain the nonlinear dependence observed in Figure 2.

Since $\Delta H°$ is relatively independent of salt concentration, decreasing absolute values of $d(1/T_m)/d \ln [Na^+]$ observed at higher Na^+ concentrations must reflect lower values of $\Delta\psi$. That is, as the sodium ion concentration of the buffer increases, absolute values of both $d(1/T_m)/d \ln [Na^+]$ and $\Delta\psi$ decrease. Since sodium ion binding to the duplex state cannot decrease with increasing bulk sodium concentration of the buffer, we propose that this observation is due to an increase in sodium ion binding to the single strands.

Analysis of eq 28 suggests that a lower boundary where eq 22 applies must exist and that eq 22 cannot apply in settings of very low Na^+ concentrations. The derivation of eq 22 yields

$$\frac{d\left(\frac{1}{T_m}\right)}{d \ln [Na^+]} = (4.29f(G{\cdot}C) - 3.95) \times 10^{-5} + 1.88 \times 10^{-5} \ln [Na^+] \quad (31)$$

In the limit as sodium ion concentration decreases to zero, the ratio on the left side of eq 31 decreases without bound. Assuming that $\Delta H°$ is independent of sodium ion concentration, eq 28 allows $\Delta\psi$ to increase without limit, which cannot be possible since the number of sodium ions bound to duplex DNA must have some maximum saturation. Therefore, eq 22 must break down as sodium concentration decreases to very low levels. As noted above further studies of our oligomer set at Na^+ concentrations below 69 mM are in progress.

It is also possible, although less likely, that the decrease of absolute value of $d(1/T_m)/d \ln [Na^+]$ at high sodium ion concentrations could be attributed to changes in water activities at high salt concentrations (*17*). Duplex DNAs have significant hydration (*21, 86*−*88*), which changes upon melting. Therefore changes in water activity with salt concentration could have an impact on melting temperatures of DNA duplex oligomers. However, the change in water activity that occurs as sodium concentration is changed from 69 mM to 1 M Na^+ is small.

Strictly speaking, $\Delta\psi$ reflects the net change in cation binding and anion exclusion with duplex formation but does not distinguish between cation uptake and anion release. Buffers used here contain coanions, mostly Cl^-, which was reported to modulate thermal stability of duplex DNAs at very high concentrations (several moles per liter) (*17*, *89*). However, it seems unlikely that chloride anions could exhibit significant effects on DNA thermal stability at concentrations below 1 M. Gruenweldel et al. (*17*) have shown that effects of LiCl and Li_2SO_4 on melting temperatures of T4 DNA are similar up to 1 M Li^+ indicating that the nature of the anion is insignificant. Record et al. (*76*) have suggested that anion effects on T_m follow the lyotropic series. Highly polarizable anions, such as CNS^- and ClO_4^-, are expected to bind more strongly to DNA and exert greater effects on T_m, while much less polarizable anions such as Cl^- have little effect on duplex stability at concentrations below 1 M.

CONCLUSIONS

The effect of sodium ion concentration on thermal stability was systematically studied for a set of 92 duplex DNA oligomers. We derived relationship 22 for scaling the T_m of DNA duplex oligomers between environments of different sodium ion concentrations. This new T_m salt correction 22 is independent of DNA concentration and length of the oligonucleotide. Equation 22 includes a dependence on oligomer sequence, specifically f(G·C), and a quadratic term that gives a better fit with the observed nonlinear T_m vs ln [Na^+] plots. The relative accuracy of our new T_m salt correction equation was compared with previously published salt corrections on two data sets: (1) a new collection of 460 T_m measurements for 92 duplex DNA oligomers reported here and (2) a set of 120 independent T_m measurements for 48 duplex DNA oligomers obtained from published sources. For both data sets, our new T_m salt correction 22 offers significantly greater accuracy than other T_m salt corrections. We underscore the general nature of this correction, which can be used to optimize a variety of probe-target hybridization systems. The new T_m salt correction 22 will be made available to all users in the OligoAnalyzer program on-line at http://www.idtdna.com/.

ACKNOWLEDGMENT

We thank Dr. Isard Dunietz for reviewing the manuscript and for helpful discussions.

SUPPORTING INFORMATION AVAILABLE

Methods for calculation of the nearest-neighbor T_m salt correction, nearest-neighbor salt correction parameters (Table S-1), results of differential scanning calorimetry experiments (Table S-2), analysis of T_m prediction errors as a function of oligomer length (Table S-3), and Figure S-1 showing reproducibility of our melting experiments. This material is available free of charge via the Internet at http://pubs.acs.org.

REFERENCES

1. Schildkraut, C., and Lifson, S. (1965) Dependence of the melting temperature of DNA on salt concentration, *Biopolymers 3*, 195−208.
2. Wetmur, J. G. (1991) DNA probes: applications of the principles of nucleic acid hybridization, *Crit. Rev. Biochem. Mol. Biol. 26*, 227−259.
3. Frank-Kamenetskii, M. D. (1971) Simplification of the empirical relationship between melting temperature of DNA, its GC content and concentration of sodium ions in solution, *Biopolymers 10*, 2623−2624.
4. Blake, R. D., and Delcourt, S. G. (1998) Thermal stability of DNA, *Nucleic Acids Res. 26*, 3323−3332 and corrigendum.
5. Marmur, J., and Doty, P. (1962) Determination of the base composition of deoxyribonucleic acid from its thermal denaturation temperature, *J. Mol. Biol. 5*, 109−118.
6. SantaLucia, J., Jr., Allawi, H. T., and Seneviratne, P. A. (1996) Improved nearest-neighbor parameters for predicting DNA duplex stability, *Biochemistry 35*, 3555−3562.

7. SantaLucia, J., Jr. (1998) A unified view of polymer, dumbbell, and oligonucleotide DNA nearest-neighbor thermodynamics, *Proc. Natl. Acad. Sci. U.S.A. 95*, 1460−1465.
8. Owczarzy, R., Vallone, P. M., Gallo, F. J., Paner, T. M., Lane, M. J., and Benight, A. S. (1997) Predicting sequence-dependent melting stability of short duplex DNA oligomers, *Biopolymers 44*, 217−239.
9. Borer, P. N., Dengler, B., Tinoco, I., Jr., and Uhlenbeck, O. C. (1974) Stability of ribonucleic acid double-stranded helices, *J. Mol. Biol. 86*, 843−853.
10. Xia, T., SantaLucia, J., Jr., Burkard, M. E., Kierzek, R., Schroeder, S. J., Jiao, X., Cox, C., and Turner, D. H. (1998) Thermodynamic parameters for an expanded nearest-neighbor model for formation of RNA duplexes with Watson−Crick base pairs, *Biochemistry 37*, 14719−14735.
11. Sugimoto, N., Nakano, S., Yoneyama, M., and Honda, K. (1996) Improved thermodynamic parameters and helix initiation factor to predict stability of DNA duplexes, *Nucleic Acids Res. 24*, 4501−4505 and corrigendum.
12. Owczarzy, R., Vallone, P. M., Goldstein, R. F., and Benight, A. S. (1999) Studies of DNA dumbbells VII: evaluation of the next-nearest-neighbor sequence-dependent interactions in duplex DNA, *Biopolymers 52*, 29−56.
13. Owen, R. J., Hill, L. R., and Lapage, S. P. (1969) Determination of DNA base compositions from melting profiles in dilute buffers, *Biopolymers 7*, 503−516.
14. Blake, R. D., and Haydock, P. V. (1979) Effect of sodium ion on the high-resolution melting of lambda DNA, *Biopolymers 18*, 3089−3109.
15. Doty, P., Boedtker, H., Fresco, J. R., Haselkorn, R., and Litt, M. (1959) Secondary structure in ribonucleic acids, *Proc. Natl. Acad. Sci. U.S.A. 45*, 482−499.
16. Gruenwedel, D. W., and Hsu, C. (1969) Salt effects on the denaturation of DNA, *Biopolymers 7*, 557−570.
17. Gruenwedel, D. W., Hsu, C., and Lu, D. S. (1971) The effects of aqueous neutral-salt solutions on the melting temperatures of deoxyribonucleic acids, *Biopolymers 10*, 47−68.
18. Gruenwedel, D. W. (1974) Salt effects on the denaturation of DNA, *Biochim. Biophys. Acta 340*, 16−30.
19. Korolev, N. I., Vlasov, A. P., and Kuznetsov, I. A. (1994) Thermal denaturation of Na- and Li-DNA in salt-free solutions, *Biopolymers 34*, 1275−1290.
20. Žaludová, R., Kleinwächter, V., and Brabec, V. (1996) The effect of ionic strength on melting of DNA modified by platinum (II) complexes, *Biophys. Chem. 60*, 135−142.
21. Spink, C. H., and Chaires, J. B. (1999) Effects of hydration, ion release, and excluded volume on the melting of triplex and duplex DNA, *Biochemistry 38*, 496−508.
22. Wells, R. D., Larson, J. E., Grant, R. C., Shortle B. E., and Cantor C. R. (1970) Physicochemical studies on polydeoxyribonucleotides containing defined repeating nucleotide sequences, *J. Mol. Biol. 54*, 465−497.
23. Elson, E. L., Scheffler, I. E., and Baldwin, R. L. (1970) Helix formation by d(TA) oligomers. III. Electrostatic effects, *J. Mol. Biol. 54*, 401−415.
24. Petruska, J., Arnheim, N., and Goodman, M. F. (1996) Stability of intrastrand hairpin structures formed by the CAG/CTG class of DNA triplet repeats associated with neurological diseases, *Nucleic Acids Res. 24*, 1992−1998.
25. Doktycz, M. J., Goldstein, R. F., Paner, T. M., Gallo, F. J., and Benight, A. S. (1992) Studies of DNA dumbbells. I. Melting curves of 17 DNA dumbbells with different duplex stem sequences linked by T_4 endloops: evaluation of the nearest-neighbor stacking interactions in DNA, *Biopolymers 32*, 849−864.
26. Erie, D. A., Jones, R. A., Olson, W. K., Sinha, N. K., and Breslauer, K. J. (1989) Melting behavior of a covalently closed, single-stranded, circular DNA, *Biochemistry 28*, 268−273.
27. Rentzeperis, D., Ho, J., and Marky, L. A. (1993) Contribution of loops and nicks to the formation of DNA dumbbells: melting behavior and ligand binding, *Biochemistry 32*, 2564−2572.
28. Williams, A. P., Longfellow, C. E., Freier, S. M., Kierzek, R., and Turner, D. H. (1989) Laser temperature-jump, spectroscopic, and thermodynamic study of salt effects on duplex formation by dGCATGC, *Biochemistry 28*, 4283−4291.
29. Nakano, S., Fujimoto, M., Hara, H., and Sugimoto, N. (1999) Nucleic acid duplex stability: influence of base composition on cation effects, *Nucleic Acids Res. 27*, 2957−2965 and personal communication.
30. Patel, D. J., and Canuel, L. L. (1979) Helix-coil transition of the self-complementary dG-dG-dA-dA-dT-dT-dC-dC duplex, *Eur. J. Biochem. 96*, 267−276.
31. Bower, M., Summers, M. F., Kell, B., Hoskins, J., Zon, G., and Wilson, W. D. (1987) Synthesis and characterization of oligodeoxyribonucleotides containing terminal phosphates. NMR, UV spectroscopic and thermodynamic analysis of duplex formation of $[d(pGGAATTCC)]_2$, $[d(GGAATTCCp)]_2$ and $[d(pGGAATTCCp)]_2$, *Nucleic Acids Res. 15*, 3531−3547.
32. Sheardy, R. D., Levine, N., Marotta, S., Suh, D., and Chaires, J. B. (1994) A thermodynamic investigation of the melting of B−Z junction forming DNA oligomers, *Biochemistry 33*, 1385−1391.
33. Bolli, M., Trafelet, H. U., and Leumann, C. (1996) Watson−Crick base-pairing properties of bicyclo-DNA, *Nucleic Acids Res. 24*, 4660−4667.
34. Tarköy, M., Bolli, M., and Leumann, C. (1994) 71. Nucleic-acid analogues with restricted conformational flexibility in the sugar−phosphate backbone ('bicyclo-DNA'), *Helv. Chim. Acta 77*, 716−744.
35. Tomac, S., Sarkar, M., Ratilainen, T., Wittung, P., Nielsen, P. E., Nordén, B., and Gräslund, A. (1996) Ionic effects on the stability and conformation of peptide nucleic acid complexes, *J. Am. Chem. Soc. 118*, 5544−5552.
36. Soto, A. M., Gmeiner, W. H., and Marky, L. A. (2002) Energetic and conformational contributions to the stability of Okazaki fragments, *Biochemistry 41*, 6842−6849 and personal communication.
37. Marky, L. A., Blumenfeld, K. S., Kozlowski, S., and Breslauer, K. J. (1983) Salt-dependent conformational transitions in the self-complementary deoxydodecanucleotide d(CGCGAATTCGCG): evidence for hairpin formation, *Biopolymers 22*, 1247−1257.
38. Kibler-Herzog, L., Zon, G., Uznanski, B., Whittier, G., and Wilson, W. D. (1991) Duplex stabilities of phosphorothioate, methylphosphonate, and RNA analogs of two DNA 14-mers, *Nucleic Acids Res. 19*, 2979−2986.
39. Breslauer, K. J. (1987) Extracting thermodynamic data from equilibrium melting curves for oligonucleotide order−disorder transitions, *Methods Enzymol. 259*, 221−242.
40. Albergo, D. D., and Turner, D. H. (1981) Solvent effects on thermodynamics of double-helix formation in $(dG\text{-}dC)_3$, *Biochemistry 20*, 1413−1418.
41. Quartin, R. S., and Wetmur, J. G. (1989) Effect of ionic strength on the hybridization of oligodeoxynucleotides with reduced charge due to methylphosphonate linkages to unmodified oligodeoxynucleotides containing the complementary sequence, *Biochemistry 28*, 1040−1047.
42. Law, S. M., Eritja, R., Goodman, M. F., and Breslauer, K. J. (1996) Spectroscopic and calorimetric characterizations of DNA duplexes containing 2-aminopurine, *Biochemistry 35*, 12329−12337.
43. Bloomfield, V. A., Crothers, D. M., and Tinoco, I., Jr. (2000) *Nucleic Acids. Structures, Properties, and Functions*, pp 307−308, University Science Books, Sausalito, CA.
44. Saiki, R. K., Gelfand, D. H., Stoffel, S., Scharf, S. J., Higuchi, R., Horn, G. T., Mullis, K. B., and Erlich, H. A. (1988) Primer-directed enzymatic amplification of DNA with a thermostable DNA polymerase, *Science 239*, 487−491.
45. Owczarzy, R. (2001) Comments on "Calculation of the energy of transition associated with inversions in double-stranded DNA" [P. Aggarwal, D. Dollimore, D. Thermochim. Acta 284 (1996) 109]: a test, *Thermochim. Acta 373*, 153−160.
46. Fasman, G. D. (Ed.) (1975) *Handbook of Biochemistry and Molecular Biology*, Vol. I, p 589, CRC Press, Boca Raton, FL.
47. Cantor, C. R., Warshaw, M. M., and Shapiro, H. (1970) Oligonucleotide interactions. III. Circular dichroism studies of the conformation of deoxyoligonucleotides, *Biopolymers 9*, 1059−1077.
48. Wartell, R. M., and Benight, A. S. (1985) Thermal denaturation of DNA molecules: a comparison of theory with experiment, *Phys. Rep. 126*, 67−107.
49. Kaiser, J. F., and Reed, W. A. (1977) Data smoothing using low-pass digital filters, *Rev. Sci. Instrum. 48*, 1447−1457.
50. Vallone, P. M., and Benight, A. S. (2000) Thermodynamic, spectroscopic, and equilibrium binding studies of DNA sequence context effects in four 40 base pair deoxyoligonucleotides, *Biochemistry 39*, 7835−7846.
51. Völker, J., Blake, R. D., Delcourt, S. G., and Breslauer, K. J. (1999) High-resolution calorimetric and optical melting profiles of DNA plasmids: resolving contributions from intrinsic melting domains and specifically designed inserts, *Biopolymers 50*, 303−318.

52. Bevington, P. R., and Robinson, D. K. (1992) *Data Reduction and Error Analysis for the Physical Sciences*, WCB/McGraw-Hill, Boston, MA.
53. Press, W. H., Teukolsky, S. A., Vetterling, W. T., and Flannery, B. P. (1996) *Numerical Recipes in Fortran 77: The Art of Scientific Computing*, Cambridge University Press, Cambridge, U.K.
54. Lawley, P. D. (1956) Interaction studies with DNA. III. The effect of changes in sodium ion concentration, pH and temperature on the ultra-violet absorption spectrum of sodium thymonucleate, *Biochim. Biophys. Acta 21*, 481−488.
55. Haschemeyer, R., Singer, B., and Fraenkel-Conrat, H. (1959) Two configurations of tobacco mosaic virus-ribonucleic acid, *Proc. Natl. Acad. Sci. U.S.A.* 45, 313−319.
56. Ivanov, I. G., and AbouHaidar, M. G. (1995) Thermal stability of oligodeoxynucleotide duplexes bound to nitrocellulose filters, *Anal. Biochem. 232*, 249−251.
57. Mehta, S., and Duncan, A. (Eds.) (2002) Improving PCR specificity. *Benchtopics in Amplification 1*, No. 3, pp 2−5, Invitrogen Corporation, Carlsbad, CA.
58. Rose, K., Mason, J. O., and Lathe, R. (2002) Hybridization parameters revisited: solutions containing SDS, *BioTechniques 33*, 54−58.
59. Rozen, S., and Skaletsky, H. J. (1998) *Primer3*, release 0.9; Whitehead Institute, Cambridge, MA. Code available at http://www-genome.wi.mit.edu/genome_software/other/primer3.html.
60. Piunno, P. A. E., Watterson, J., Wust, C. C., and Krull, U. J. (1999) Considerations for the quantitative transduction of hybridization of immobilized DNA, *Anal. Chim. Acta 400*, 73−89.
61. Le Novère, N. (2001) MELTING, computing the melting temperature of nucleic acid duplex, *Bioinformatics 17*, 1226−1227.
62. Rychlik, W., Spencer, W. J., and Rhoads, R. E. (1990) Optimization of the annealing temperature for DNA amplification in vitro, *Nucleic Acids Res. 18*, 6409−6412.
63. Peyret, N. (2000) Prediction of Nucleic Acid Hybridization: Parameters and Algorithms, Ph.D. Thesis, Wayne State University, Detroit, MI.
64. Chiu, W. L. A. K., Sze, C. N., Ip, L. N., Chan, S. K., and Au-Yeung, S. C. F. (2001) NTDB: Thermodynamic Database for Nucleic Acids, *Nucleic Acids Res. 29*, 230−233.
65. Vyazovkina, E. V., Savchenko, E. V., Lokhov, S. G., Engels, J. W., Wickstrom, E., and Lebedev, A. V. (1994) Synthesis of specific diastereomers of a DNA methylphosphonate heptamer, d(CpCpApApApCpA), and stability of base pairing with the normal DNA octamer d(TpGpTpTpTpGpGpC), *Nucleic Acids Res. 22*, 2404−2409.
66. Braunlin, W. H., and Bloomfield, V. A. (1991) ^{1}H NMR study of the base-pairing reactions of d(GGAATTCC): salt effects on the equilibria and kinetics of strand association, *Biochemistry 30*, 754−758.
67. Mokhir, A. A., and Richert, C. (2000) Synthesis and monitored selection of 5′-nucleobase-capped oligodeoxyribonucleotides, *Nucleic Acids Res. 28*, 4254−4265.
68. Sabahi, A., Guidry, J., Inamati, G. B., Manoharan, M., and Wittung-Stafshede, P. (2001) Hybridization of 2′-ribose modified mixed-sequence oligonucleotides: thermodynamic and kinetic studies, *Nucleic Acids Res. 29*, 2163−2170.
69. Hashimoto, H., Nelson, M. G., and Switzer, C. (1993) Zwitterionic DNA, *J. Am. Chem. Soc. 115*, 7128−7134.
70. Jung, K., and Switzer, C. (1994) 2′,5′-DNA containing guanine and cytosine forms stable duplexes, *J. Am. Chem. Soc. 116*, 6059−6061.
71. Hildbrand, S., and Leumann, C. (1996) Enhancing DNA triple helix stability at neutral pH by the use of oligonucleotides containing a more basic deoxycytidine analogue, *Angew. Chem., Int. Ed. Engl. 35*, 1968−1970.
72. Sund, C., Puri, N., and Chattopadhyaya, J. (1996) Synthesis of C-branched spermine tethered oligo-DNA and the thermal stability of the duplexes and triplexes, *Tetrahedron 52*, 12275−12290.
73. Goldstein, R. F., and Benight, A. S. (1992) How many numbers are required to specify sequence-dependent properties of polynucleotides? *Biopolymers 32*, 1679−1693.
74. Gray, D. M. (1997) Derivation of nearest-neighbor properties from data on nucleic acid oligomers, *Biopolymers 42*, 783−793.
75. Record, M. T., Jr., and Lohman, T. M. (1978) A semiempirical extension of polyelectrolyte theory to the treatment of oligoelectrolytes: application to oligonucleotide helix-coil transitions, *Biopolymers 17*, 159−166.
76. Record, M. T., Jr., Anderson, C. F., and Lohman, T. M. (1978) Thermodynamic analysis of ion effects on the binding and conformational equilibria of proteins and nucleic acids: the roles of ion association or release, screening, and ion effects on water activity, *Q. Rev. Biophys. 2*, 103−178.
77. Manning, G. S. (1972) On the application of polyelectrolyte "limiting laws" to the helix-coil transition of DNA, *Biopolymers 11*, 937−949.
78. Anderson, C. F., and Record, M. T., Jr. (1995) Salt-nucleic acid interactions, *Annu. Rev. Phys. Chem. 46*, 657−700.
79. Cahen, P., Luhmer, M., Fontaine, C., Morat, C., Reisse, J., and Bartik, K. (2000) Study by ^{23}Na-NMR, ^{1}H-NMR, and ultraviolet spectroscopy of the thermal stability of an 11-basepair oligonucleotide, *Biophys. J. 78*, 1059−1069.
80. Ascoli, F., Botré, C., and Liquori, A. M. (1961) Irreversible changes of ionic activities following thermal denaturation of sodium deoxyribonucleate, *J. Mol. Biol. 3*, 202−207.
81. Inman, R. B., and Jordan, D. O. (1960) Deoxypentose nucleic acids. XII. The denaturation of deoxyribonucleic acid in aqueous solution: changes produced by environment, *Biochim. Biophys. Acta 42*, 427−434.
82. Völker, J., Klump, H. H., Manning, G. S., and Breslauer, K. J. (2001) Counterion association with native and denatured nucleic acids: an experimental approach, *J. Mol. Biol. 310*, 1011−1025.
83. Olmsted, M. C., Anderson, C. F., and Record, M. T., Jr. (1991) Importance of oligoelectrolyte end effects for the thermodynamics of conformational transitions of nucleic acid oligomers: a grand canonical Monte Carlo analysis, *Biopolymers 31*, 1593−1604.
84. Manning, G. S., and Mohanty, U. (1997) Counterion condensation on ionic oligomers, *Physica A 247*, 196−204.
85. Weast, R. C. (Ed.) (1984) *CRC Handbook of Chemistry and Physics*, p D-173, CRC Press, Boca Raton, FL.
86. Chalikian, T. V., Völker, J., Srinivasan, A. R., Olson, W. K., and Breslauer, K. J. (1999) The hydration of nucleic acid duplexes as assessed by a combination of volumetric and structural techniques, *Biopolymers 50*, 459−471.
87. Egli, M., Tereshko, V., Teplova, M., Minasov, G., Joachimiak, A., Sanishvili, R., Weeks, C. M., Miller, R., Maier, M. A., An, H., Cook, P. D., and Manoharam, M. (1998) X-ray crystallographic analysis of the hydration of A- and B-form DNA at atomic resolution, *Biopolymers 48*, 234−252.
88. Soto, A. M., Kankia, B. I., Dande, P., Gold, B., and Marky, L. A. (2002) Thermodynamic and hydration effects for the incorporation of a cationic 3-aminopropyl chain into DNA, *Nucleic Acids Res. 30*, 3171−3180.
89. Hamaguchi, K., and Geiduschek, E. P. (1962) The effect of electrolytes on the stability of the deoxyribonucleate helix, *J. Am. Chem. Soc. 84*, 1329−1338.
90. Privalov, P. L., Ptitsyn, O. B., and Birshtein, T. M. (1969) Determination of stability of the DNA double helix in an aqueous medium, *Biopolymers 8*, 559−571.
91. Karapetian, A. T., Vardevanian, P. O., and Frank-Kamenetskii, M. D. (1990) Enthalpy of helix-coil transition of DNA: dependence on Na^+ concentration and GC-content, *J. Biomol. Struct. Dyn. 8*, 131−138.
92. Laing, L. G., Gluick, T. C., and Draper, D. E. (1994) Stabilization of RNA structure by Mg ions, *J. Mol. Biol. 237*, 577−587.
93. Bond, J. P., Anderson, C. F, and Record, M. T., Jr. (1994) Conformational transitions of duplex and triplex nucleic acid helices: Thermodynamic analysis of effects of salt concentration on stability using preferential interaction coefficients, *Biophys. J. 67*, 825−836.
94. Record, M. T., Jr, Zhang, W., and Anderson, C. F. (1998) Analysis of effects of salts and uncharged solutes on protein and nucleic acid equilibria and processes: A practical guide to recognizing and interpreting polyelectrolyte effects, Hofmeister effects, and osmotic effects of salts, *Adv. Protein Chem. 51*, 281−353.

BI034621R